International Journal of Structural Stability and Dynamics
Vol. 15, No. 2 (2015) 1450041 (37 pages)

DOI: 10.1142/S0219455414500412

World Scientific
www.worldscientific.com

Damping Effect of Pendulum Tuned Mass Damper on Vibration of Two-Dimensional Rigid Body

Yi-Ren Wang* and Ko-En Hung

Department of Aerospace Engineering, Tamkang University
NewTaipei City, Tamsui Dist., Taiwan 25137, R.O.C.
**090730@mail.tku.edu.tw*

Received 9 January 2014
Accepted 9 June 2014
Published 16 July 2014

This study investigated the effect of a pendulum tuned mass damper (PTMD) on the vibration of a slender two-dimensional (2D) rigid body with 1:2 internal resonance. Focus is placed on the damping effect of various parameters of the PTMD on preventing the internal resonance of the system. The instruments used include fixed points plots, time response and Poincaré maps, which were compared for confirmation of accuracy. The Lagrange's equation is employed to derive the equations of motion for the system. The method of multiple scales (MOMS) is applied to analyzing this nonlinear vibration model. The internal resonance conditions of the rigid body in vibration are obtained by the eigenanalysis. Moreover, a 3D internal resonance contour plot (3D-IRCP) aided by various amplitude analysis tables is proposed for identification of the parameter combinations of the PTMD for preventing internal resonance. This approach enables the designers to evaluate the effectiveness of various parameter combinations of the PTMD prior to the design process. The present study indicates that without changing the main configuration, the vibration amplitudes in the main body can be greatly reduced under certain parameter combinations of the PTMD.

Keywords: Tuned mass damper; vibration reduction; nonlinear vibration; internal resonance.

1. Introduction

Vibration in mechanical systems is unavoidable, often resulting in the loosening of components, fatigue and structural damage. As a result, the need to identify proper means of dampening vibration remains a challenge for engineers. Among the many methods of vibration reduction, passive dampers are the most widely used, due to their simplicity and low cost. But in some situations, they tend to be less effective than the active counterparts. In this study, the conventional passive damper is

*Corresponding author.

modified as a pendulum tuned mass damper (PTMD), referred to as the pendulum vibration absorber (PVA), taking into account various damping effects. With the premise of preserving the original vibration configuration, the optimal damping effects are achieved without excessive cost, simply by adjusting the location, mass, and modulus of elasticity of the PTMD.

The tuned mass damper (TMD) is the most common approach to vibration absorption. The concept was first proposed by Ormondroyd and Den Hartog[1] in 1928, following which a wide range of applications emerged. Vakakis and Paipetis[2] studied the damping effects of a TMD with a single degree of freedom (SDOF) on the first mode of a vibrating body with multiple DOFs. ASUS[3] also applied the TMD to the development of a dynamic damper system for their CD-ROM drives. Zuo and Nayfeh[4] reported that a single damper with two degrees of freedom (2DOFs) can provide better damping effect in the first two flexural modes of a free–free beam than what would be possible using a single damper with SDOF or even two SDOF dampers. Understanding this principle has provided the opportunity to design more effective vibration absorbers (dampers). Generally, dampers have been used to reduce vibration in a single direction; however, Almazán *et al.*[5] presented a bi-direction TMD capable of reducing transverse and rotational vibrations, as well as vibrations in other directions.

To maintain the configuration of the main body, such that merely altering the location of the dampers can achieve the effect of vibration reduction, Wang and Chen[6] proposed position optimization of a mass-spring-damper vibration absorber for a rotating mechanisms (such as optical disk drives, rotary-wings and deck coupled systems). Wang and Chang[7] studied the problem of nonlinear vibration in a rigid body plate. Each of the four corners of the plate was supported by a nonlinear spring to simulate the transverse-rotate-rotate nonlinear vibrations with two point-mass shock absorbers suspended beneath the body. The positions of the two absorbers can be adjusted to achieve the best vibration reduction effect. Recently, Wang and Lin[8] examined how vibration absorbers influence the stability of nonlinear flow-solid interaction systems. A novel approach was proposed in which both an internal resonance contour plot (IRCP) and flutter speed contour plot (FSCP) were used for the analysis of nonlinear dynamic stability. Meanwhile, they demonstrated that identifying the optimal location for the damper can reduce vibration, an insight which forms the inspiration of this study.

PTMD has been widely applied in engineering vibration problems. For example, TMDs have been installed in tall buildings to reduce wind-induced sway as well as for protection from seismic events.[9] Absorbers can be mounted on the rotor blades of a helicopter for attenuation of aerodynamically induced vibrations.[10] Wu[11] used an active rotational PVA to reduce the transverse vibration of a primary body. Varying the rotational speed of the pendulum enables the tuning of the absorber frequency, whereupon the inertial force of the revolving mass is helpful in reducing vibration of the main body. These results have been improved upon in subsequent

studies.[12,13] A linear SDOF vibration system coupled with a parallel attached nonlinear autoparametric PVA was considered by Vyas and Bajaj[14] in their study of 1:1 and 1:2 internal resonances between the pendulum and primary oscillator. The idea of a multiple array of auto-parametric absorbers has been suggested and its effectiveness in enhancing the absorber bandwidth has been analytically demonstrated.

Nayfeh[15] described a number of nonlinear vibration systems, including the Lindstedt–Poincaré method, the method of multiple scales (MOMS), and the method of averaging. MOMS is more convenient for the analysis of general nonlinear vibration systems with damping; for this reason it is adopted in the analysis of this study. Ji and Zu[16] investigated the shaft system of a Timoshenko beam and employed the MOMS to calculate the natural frequency of the nonlinear system and analyze its steady state responses. Chao *et al.*[17] examined the automatic ball-type balancer system (ABS) installed on optical disk drives (ODD), taking into account the relative torsional motion between the ODD case and the spindle-disk-ABS-turntable system. They also used the MOMS to analyze a steady state solution and achieved a significant reduction in vibration.

In most of the existing works, either SDOF passive TMDs or active vibration absorbers were indestigated. In this study, a PTMD was hung beneath the vibrating main body with a coupled nonlinear extension and torsion spring, functioning as 2DOFs in the transverse and rotational directions. The main body vibration can be absorbed in both the transverse and rotational directions simultaneously. A new concept of 3D-IRCP was introduced to avoid main system internal resonance for preliminary design of the PTMD. The Lagrange's method was employed to derive the equations of motion for the system and the MOMS was applied to dividing the equations into multiple scales. Using the eigen-analysis, the internal resonance conditions of the vibrating body were obtained. Under the circumstances of internal resonance, the PTMD was suspended at various locations beneath the vibrating body for studying the effect of various combinations of the damper mass ratio ($\bar{m}$), extension spring constant ($\hat{k}_S$), and torsion spring constant ($\hat{k}_T$) in preventing the internal resonance, while reducing the system vibration. The fixed points plots, along with numerical analysis, were used to verify the accuracy of the frequency response and time response calculated.

2. Theoretical Model

In this study, a slender rigid body with 2DOFs is considered, which is supported by a nonlinear spring with a linear damper at both ends, as shown in Fig. 1. Beneath the main body, a PTMD is suspended by a coupled nonlinear torsion spring and extension spring, which can move in the transverse direction as well as rotate. Generally, when a simple pendulum is suspended beneath a body with a hinge, its oscillating behavior will not be coupled with the main body. This is because the hinge support can theoretically bear forces only in the vertical and horizontal directions,

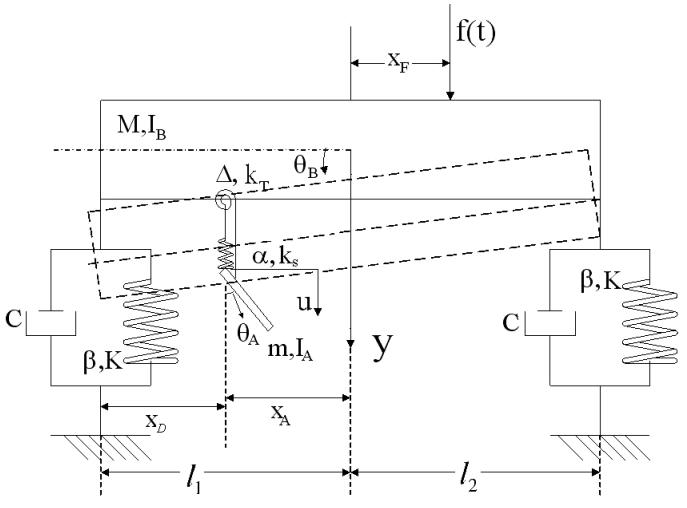

Fig. 1. Schematic diagram of the model.

but cannot resist moment, and thus, the oscillation of the PTMD itself won't affect the rotation of the vibrating body. For this reason, a torsion spring and an extension spring are installed at the point where the PTMD connects with the main body to provide the transverse and rotational coupling effects. We used M and m to denote the masses of the main body and PTMD, respectively. The transverse displacement and rotation of the main body were represented by y and θ_B, whereas the transverse displacement and rotation of the PTMD were represented by u and θ_A. The system has a total of 4DOFs. The relevant parameters are defined as follows: $K =$ the linear spring coefficient of the extension springs supporting the two ends of the main body; $\beta =$ the nonlinear spring coefficient; $C =$ the coefficient of the linear damper; $k_T =$ the coefficient of the torsion spring connecting the PTMD to the main body, $\Delta =$ the coefficient of the nonlinear torsion spring; $k_S =$ the coefficient of the extension spring connecting the PTMD to the main body, $\alpha =$ the nonlinear extension spring coefficient; I_B and I_A denote the moment of inertia in the main body and the PTMD, respectively; $l_1 =$ the center of mass of the main body, and x_D and x_A denote the location of the PTMD. Furthermore, $f =$ the harmonic force exerted on the system, and $x_F =$ the distance between the external force and center of mass.

The Lagrange method is employed to derive equations of motion for the system. The kinetic energy, potential energy, dissipation energy, and generalized coordinates are denoted by T, V, R and q_i, respectively, and the 4-DOFs of the system are y, θ_B, u and θ_A. Lagrange's equation is as follows:

$$\frac{d}{dt}\left(\frac{\partial T}{\partial \dot{q}_i}\right) - \frac{\partial T}{\partial q_i} + \frac{\partial R}{\partial \dot{q}_i} + \frac{\partial V}{\partial q_i} = Q_i^{(n)}, \quad (i = 1 \sim n), \tag{1}$$

where

$$T = \frac{1}{2}M\dot{y}^2 + \frac{1}{2}m\left[\left(-\frac{l_A}{2}\dot{\theta}_A\cos\theta_A\right)^2 + \left(\dot{u} - \frac{l_A}{2}\dot{\theta}_A\sin\theta_A\right)^2\right] + \frac{1}{2}I_A\dot{\theta}_A^2 + \frac{1}{2}I_B\dot{\theta}_B^2, \tag{2}$$

$$\begin{aligned} V = {} & \frac{1}{2}K[(y + l_1\sin\theta_B) + \beta(y + l_1\sin\theta_B)^3]^2 \\ & + \frac{1}{2}K[(y - l_2\sin\theta_B) + \beta(y - l_2\sin\theta_B)^3]^2 \\ & + \frac{1}{2}k_T[(\theta_A - \theta_B) + \Delta(\theta_A - \theta_B)^3]^2 \\ & + \frac{1}{2}k_S\{[u - (y + x_A\sin\theta_B)] \\ & + \alpha[u - (y + x_A\sin\theta_B)]^3\}^2 + mg\frac{l_A}{2}(1 - \cos\theta_A), \end{aligned} \tag{3}$$

$$R = \frac{1}{2}C[(\dot{y} + \dot{\theta}_B l_1\cos\theta_B)^2 + (\dot{y} - \dot{\theta}_B l_2\cos\theta_B)^2]. \tag{4}$$

Substituting T, V and R, into Eq. (1), one can obtain the equations for the 4DOFs:

Equation of motion for the main body in the transverse direction:

$$\begin{aligned} & M\ddot{y} + C(2\dot{y} + \dot{\theta}_B l_1\cos\theta_B - \dot{\theta}_B l_2\cos\theta_B) + K[(y + l_1\sin\theta_B) + 4\beta(y + l_1\sin\theta_B)^3] \\ & \quad + K[(y - l_2\sin\theta_B) + 4\beta(y - l_2\sin\theta_B)^3] + k_S[(-u + y + x_A\sin\theta_B) \\ & \quad + 4\alpha(-u + y + x_A\sin\theta_B)^3] = f. \end{aligned} \tag{5}$$

Equation of motion for rotation of the main body:

$$\begin{aligned} & I_B\ddot{\theta}_B + C\cos\theta_B[l_1(\dot{y} + \dot{\theta}_B l_1\cos\theta_B) - l_2(\dot{y} - \dot{\theta}_B l_2\cos\theta_B)] \\ & \quad + \frac{1}{2}K[(l_1^2\sin 2\theta_B + 2l_1 y\cos\theta_B) + 2\beta(4l_1^4\theta_B^3 + 12l_1^3 y\theta_B^2 + 12l_1^2 y^2\theta_B + 4l_1 y^3)] \\ & \quad + \frac{1}{2}K[(l_2^2\sin 2\theta_B - 2l_2 y\cos\theta_B) + 2\beta(4l_2^4\theta_B^3 - 12l_2^3 y\theta_B^2 + 12l_2^2 y^2\theta_B - 4l_2 y^3)] \\ & \quad - k_T[(\theta_A - \theta_B) + 4\Delta(\theta_A - \theta_B)^3] \\ & \quad + \frac{1}{2}k_S[(-2ux_A\cos\theta_B + 2x_A y\cos\theta_B + x_A^2\sin 2\theta_B) \\ & \quad + 2\beta(-2ux_A\cos\theta_B + 2x_A y\cos\theta_B + x_A^2\sin 2\theta_B)^3] = M_{\theta_B}. \end{aligned} \tag{6}$$

Equation of motion for the PTMD in the transverse direction:

$$\begin{aligned} & m\left[\ddot{u} - \frac{l_A}{2}(\ddot{\theta}_A\sin\theta_A + \dot{\theta}_A^2\cos\theta_A)\right] + k_S\{[u - (y + x_A\sin\theta_B)] \\ & \quad + 4\alpha[u - (y + x_A\sin\theta_B)]^3\} = 0. \end{aligned} \tag{7}$$

Equation of motion for rotation of the PTMD:

$$\frac{1}{2}m\left[\frac{l_A^2}{2}\ddot{\theta}_A - l_A(\ddot{u}\sin\theta_A + \dot{u}\dot{\theta}_A\cos\theta_A)\right] + I_A\ddot{\theta}_A + \frac{1}{2}ml_A\dot{u}\dot{\theta}_A\cos\theta_A + k_T[(\theta_A-\theta_B)+4\Delta(\theta_A-\theta_B)^3] + mg\frac{l_A}{2}\sin\theta_A = 0. \tag{8}$$

To facilitate solution of the above equations of motion, the Taylor series expansion (to the third-order terms) is adopted for the trigonometric functions. The expanded equations of motion are then nondimensionalized. The definitions of the dimensionless coefficients and variables are presented in Appendix A. Furthermore, we set the scales of all the nonlinear terms and external force terms as ε^1 to facilitate the perturbation analysis. The results of the dimensionless equations of motion are as follows.

Equation of motion for the main body in the transverse direction:

$$\begin{aligned}
&\frac{d^2\bar{y}}{d\tau^2} + \bar{y} + \hat{k}_s\bar{y} + \frac{\bar{l}_1-\bar{l}_2}{2}\theta_B + \hat{k}_s\bar{x}_A\theta_B - \hat{k}_s\bar{u} + \varepsilon\Bigg(\xi_y\frac{d\bar{y}}{d\tau} + \frac{\xi_y}{2}\frac{d\theta_B}{d\tau}(\bar{l}_1-\bar{l}_2) \\
&- \frac{\xi_y}{4}\frac{d\theta_B}{d\tau}\theta_B^2(\bar{l}_1-\bar{l}_2) - 12\bar{\alpha}\hat{k}_s\bar{x}_A^2\bar{u} - 24\hat{k}_s\bar{\alpha}\bar{x}_A\bar{y}\theta_B\bar{u} + 6\bar{\beta}\bar{y}\theta_B^2(\bar{l}_1^2+\bar{l}_2^2) \\
&+ 12\hat{k}_s\bar{\alpha}\bar{x}_A^2\bar{y}\theta_B^2 + 12\hat{k}_s\bar{\alpha}\bar{y}\bar{u}^2 + (6\bar{\beta}(\bar{l}_1-\bar{l}_2) + 12\hat{k}_s\bar{\alpha}\bar{x}_A)\bar{y}^2\theta_B \\
&- 12\hat{k}_s\bar{\alpha}\bar{y}^2\bar{u} + 12\hat{k}_s\bar{\alpha}\bar{x}_A\theta_B\bar{u}^2 - 12\hat{k}_s\bar{\alpha}\bar{x}_A^2\theta_B^2\bar{u} + (4\bar{\beta}+4\hat{k}_s\bar{\alpha})\bar{y}^3 + \Bigg(2\bar{\beta}(\bar{l}_1^3-\bar{l}_2^3) \\
&- \frac{\bar{l}_1-\bar{l}_2}{12} - \frac{1}{6}\hat{k}_s\bar{x}_A + 4\hat{k}_s\bar{\alpha}\bar{x}_A^3\Bigg)\theta_B^3 - 4\hat{k}_s\bar{\alpha}\bar{u}^3\Bigg) = \varepsilon\bar{f}_y.
\end{aligned} \tag{9}$$

Equation of motion for rotation of the main body:

$$\begin{aligned}
&\frac{d^2\theta_B}{d\tau^2} + (\bar{\omega}_{\theta_B}^2(\bar{l}_1-\bar{l}_2) + 6\hat{k}_s\bar{x}_A)\bar{y} + (\bar{\omega}_{\theta_B}^2(\bar{l}_1^2+\bar{l}_2^2) + 6\hat{k}_s\bar{x}_A^2 + 12\hat{k}_T)\theta_B - 6\hat{k}_s\bar{x}_A\bar{u} \\
&- 12\hat{k}_T\theta_A + \varepsilon\Bigg(\xi_{\theta_B}\frac{d\bar{y}}{d\tau}(\bar{l}_1-\bar{l}_2) - \xi_{\theta_B}\frac{d\bar{y}}{d\tau}\frac{\theta_B^2}{2}(\bar{l}_1-\bar{l}_2) + \xi_{\theta_B}\frac{d\theta_B}{d\tau}(\bar{l}_1^2+\bar{l}_2^2) \\
&- \xi_{\theta_B}\theta_B^2\frac{d\theta_B}{d\tau}(\bar{l}_1^2+\bar{l}_2^2) - 48\bar{\omega}_{\theta_B}^2\hat{k}_s\bar{\beta}\bar{x}_A^2\bar{y}\theta_B\bar{u} + (12\bar{\omega}_{\theta_B}^2\bar{\beta}(\bar{l}_1^3+\bar{l}_2^3) + 24\bar{\omega}_{\theta_B}^2\hat{k}_s\bar{\beta}\bar{x}_A^3 \\
&- \frac{1}{2}\bar{\omega}_{\theta_B}^2(\bar{l}_1-\bar{l}_2) - 3\hat{k}_s\bar{x}_A)\bar{y}\theta_B^2 + 24\bar{\omega}_{\theta_B}^2\hat{k}_s\bar{\beta}\bar{x}_A\bar{y}\bar{u}^2 + 24\bar{\omega}_{\theta_B}^2\hat{k}_s\bar{\beta}\bar{x}_A^2\theta_B\bar{u}^2 \\
&+ 48\hat{k}_T\bar{\Delta}\theta_B\theta_A^2 + (-24\bar{\omega}_{\theta_B}^2\hat{k}_s\bar{\beta}\bar{x}_A^3 + 3\hat{k}_s\bar{x}_A)\theta_B^2\bar{u} - 48\hat{k}_T\bar{\Delta}\theta_B^2\theta_A \\
&+ (12\bar{\omega}_{\theta_B}^2\bar{\beta}(\bar{l}_1^2+\bar{l}_2^2) + 24\bar{\omega}_{\theta_B}^2\hat{k}_s\bar{\beta}\bar{x}_A^2)\bar{y}^2\theta_B - 24\bar{\omega}_{\theta_B}^2\hat{k}_s\bar{\beta}\bar{x}_A\bar{y}^2\bar{u} \\
&+ (4\bar{\omega}_{\theta_B}^2\bar{\beta}(\bar{l}_1+\bar{l}_2) + 8\bar{\omega}_{\theta_B}^2\hat{k}_s\bar{\beta}\bar{x}_A)\bar{y}^3 + (4\bar{\omega}_{\theta_B}^2\bar{\beta}(\bar{l}_1^4+\bar{l}_2^4) - 4\hat{k}_s\bar{x}_A^2 \\
&- \frac{2}{3}\bar{\omega}_{\theta_B}^2(\bar{l}_1^2+\bar{l}_2^2) + 48\hat{k}_T\bar{\Delta})\theta_B^3 - 8\bar{\omega}_{\theta_B}^2\hat{k}_s\bar{\beta}\bar{x}_A\bar{u}^3 - 48\hat{k}_T\bar{\Delta}\theta_A^3\Bigg) = \varepsilon\bar{M}_{\theta_B}.
\end{aligned} \tag{10}$$

Equation of motion for the PTMD in the transverse direction:

$$\frac{d^2\bar{u}}{d\tau^2} - \bar{\omega}_u^2(\bar{y}-\bar{u}) - \bar{\omega}_u^2\bar{x}_A\theta_B + \varepsilon\left(-\frac{\bar{l}_A}{2}\frac{d^2\theta_A}{d\tau^2}\theta_A - \frac{\bar{l}_A}{2}\left(\frac{d\theta_A}{d\tau}\right)^2 + 24\bar{\omega}_u^2\bar{\alpha}\bar{x}_A\bar{y}\theta_B\bar{u}\right.$$
$$- 12\bar{\omega}_u^2\bar{\alpha}\bar{x}_A^2\bar{y}\theta_B^2 - 12\bar{\omega}_u^2\bar{\alpha}\bar{y}\bar{u}^2 - 12\bar{\omega}_u^2\bar{\alpha}\bar{x}_A^2\bar{y}^2\theta_B + 12\bar{\omega}_u^2\bar{\alpha}\bar{y}^2\bar{u} - 12\bar{\omega}_u^2\bar{\alpha}\bar{x}_A\theta_B\bar{u}^2$$
$$\left. + 12\bar{\omega}_u^2\bar{\alpha}\bar{x}_A^2\theta_B^2\bar{u} - 4\bar{\omega}_u^2\bar{\alpha}\bar{y}^3 + \left(4\bar{\omega}_u^2\bar{\alpha}\bar{x}_A^3 + \frac{1}{6}\bar{\omega}_u^2\bar{x}_A\right)\theta_B^3 + 4\bar{\omega}_u^2\bar{\alpha}\bar{u}^3\right) = 0. \tag{11}$$

Equation of motion for rotation of the PTMD:

$$\frac{d^2\theta_A}{d\tau^2} - \bar{\omega}_{\theta_A}^2\theta_B + \left(\bar{\omega}_{\theta_A}^2 + \frac{3}{2}\bar{\omega}_{PD}^2\right)\theta_A + \varepsilon\left(-\frac{3}{2\bar{l}_A}\frac{d^2\bar{u}}{d\tau^2}\theta_A - 12\bar{\omega}_{\theta_A}^2\bar{\Delta}\theta_B\theta_A^2\right.$$
$$\left. + 12\bar{\omega}_{\theta_A}^2\bar{\Delta}\theta_B^2\theta_A - 4\bar{\omega}_{\theta_A}^2\bar{\Delta}\theta_B^3 + \left(4\bar{\omega}_{\theta_A}^2\bar{\Delta} - \frac{1}{4}\bar{\omega}_{PD}^2\right)\theta_A^3\right) = 0. \tag{12}$$

An observation of Eqs. (9) and (10) reveals that, although the dimensionless coefficient $\hat{k}_T$ of the torsion spring connecting the PTMD and main body does not influence the displacement of the main body in the transverse direction, it exerts a degree of influence on the rotation of the main body (θ_B). In the linear portion of Eq. (10) (the first five terms), the scope of the influence from $\hat{k}_T$ is limited to the rotation of the main body (θ_B, the third item on the left-hand side of Eq. (10) $((\bar{\omega}_{\theta_B}^2(\bar{l}_1^2+\bar{l}_2^2) + 6\hat{k}_S\bar{x}_A^2 + 12\hat{k}_T)\theta_B)$) and the PTMD ($\theta_A$, the fifth item on the left-hand side of Eq. (10) $(-12\hat{k}_T\theta_A)$). In addition, the coefficient in the front is fixed ($12\hat{k}_T$), indicating that the influence of $\hat{k}_T$ does not change with the location of the PTMD. However, looking at the θ_A in the fifth term ($12\hat{k}_T\theta_A$) on the left-hand side of Eq. (10), we observe that the factors determining θ_A still lie in the equation of motion for rotation in the damper, Eq. (12), where a number of influential factors can be found (such as $\bar{m}$ and l_A). The nonlinear portion of Eq. (10) also shows the products of $\hat{k}_T$ and θ_A as well as $\hat{k}_T$ and θ_B, which makes this nonlinear problem even more complex. Not only is the linear equation unable to predict the influence of the various parameters, but the results cannot be understood simply by glimpsing a single equation of motion. The dimensionless extension spring constant ($\hat{k}_S$) influences $\bar{y}$, θ_B and the multiplying variable $\bar{x}_A$, which indicates that the location of the PTMD and the value of $\hat{k}_S$ both influence the vibration of the main body. These factors will be discussed at length in Sec. 4.

To facilitate analysis of the conditions capable of reducing internal resonance in the main body, as well as the frequency responses of the main body when there is no PTMD, one can choose to eliminate the equations of motion for the PTMD, thereby deriving the following equations of motion for the main body:

Dimensionless equation of motion for the main body in the transverse direction:

$$\frac{d^2\bar{y}}{d\tau^2}+\bar{y}+\frac{\bar{l}_1-\bar{l}_2}{2}\theta_B+\varepsilon\Bigg(\xi_y\frac{d\bar{y}}{d\tau}+\frac{\xi_y}{2}\frac{d\theta_B}{d\tau}(\bar{l}_1-\bar{l}_2)-\frac{\xi_y}{4}\frac{d\theta_B}{d\tau}\theta_B^2(\bar{l}_1-\bar{l}_2)+6\bar{\beta}(\bar{l}_1^2+\bar{l}_2^2)\bar{y}\theta_B^2+6\bar{\beta}(\bar{l}_1-\bar{l}_2)\bar{y}^2\theta_B+4\bar{\beta}\bar{y}^3+\left(2\bar{\beta}(\bar{l}_1^3-\bar{l}_2^3)-\frac{\bar{l}_1-\bar{l}_2}{12}\right)\theta_B^3\Bigg)=\varepsilon\bar{f}_y. \tag{13}$$

Dimensionless equation of motion for rotation of the main body:

$$\begin{aligned}\frac{d^2\theta_B}{d\tau^2}&+\bar{\omega}_{\theta_B}^2(\bar{l}_1-\bar{l}_2)\bar{y}+\bar{\omega}_{\theta_B}^2(\bar{l}_1^2+\bar{l}_2^2)\theta_B+\varepsilon\Bigg(\xi_{\theta_B}\frac{d\bar{y}}{d\tau}(\bar{l}_1-\bar{l}_2)-\xi_{\theta_B}\frac{d\bar{y}}{d\tau}\frac{\theta_B^2}{2}(\bar{l}_1-\bar{l}_2)\\&+\xi_{\theta_B}\frac{d\theta_B}{d\tau}(\bar{l}_1^2+\bar{l}_2^2)-\xi_{\theta_B}\theta_B^2\frac{d\theta_B}{d\tau}(\bar{l}_1^2+\bar{l}_2^2)\\&+\left(-\bar{\omega}_{\theta_B}^2\frac{(\bar{l}_1-\bar{l}_2)}{2}+12\bar{\omega}_{\theta_B}^2\beta(\bar{l}_1^3+\bar{l}_2^3)\right)\bar{y}\theta_B^2\\&+12\bar{\omega}_{\theta_B}^2\bar{\beta}(\bar{l}_1^2+\bar{l}_2^2)\bar{y}^2\theta_B+4\bar{\omega}_{\theta_B}^2\bar{\beta}(\bar{l}_1+\bar{l}_2)\bar{y}^3+\Bigg(4\bar{\omega}_{\theta_B}^2\bar{\beta}(\bar{l}_1^4+\bar{l}_2^4)\\&-\frac{2}{3}\bar{\omega}_{\theta_B}^2(\bar{l}_1^2+\bar{l}_2^2)\Bigg)\theta_B^3\Bigg)=\varepsilon\bar{M}_{\theta_B}.\end{aligned} \tag{14}$$

Analysis of Eqs.(13) and (14) will be presented in Sec. 3.2.

3. Analysis of Nonlinear System

3.1. *System with PTMD*

The MOMS is adopted to divide the nonlinear equations of motion into two different time scales. Let $T_0=\tau$ for fast time change terms and $T_1=\varepsilon\tau$ for slow time change terms; ε served as a small parameter for perturbation analysis. The approximation to the solutions can be expressed as follows:

$$\begin{aligned}\bar{y}(\tau,\varepsilon)&=\varepsilon^0\bar{y}_0(T_0,T_1)+\varepsilon^1\bar{y}_1(T_0,T_1),\\\theta_B(\tau,\varepsilon)&=\varepsilon^0\theta_{B0}(T_0,T_1)+\varepsilon^1\theta_{B1}(T_0,T_1),\\\bar{u}(\tau,\varepsilon)&=\varepsilon^0\bar{u}_0(T_0,T_1)+\varepsilon^1\bar{u}_1(T_0,T_1),\\\theta_A(\tau,\varepsilon)&=\varepsilon^0\theta_{A0}(T_0,T_1)+\varepsilon^1\theta_{A1}(T_0,T_1).\end{aligned}$$

For the sake of conciseness, we simplify the equations and present the coefficients in letters, the details of which are presented in Appendix B. As ε is a small value, we ignore ε terms with orders equal to or greater than 2. Therefore, using MOMS, the equations of motion for the system (Eqs. (9)–(12)) can be divided into:

Equations containing ε^0:

$$P_1\frac{\partial^2}{\partial T_0^2}\bar{y}_0+P_9\bar{y}_0+P_{10}\theta_{B0}+P_{11}\bar{u}_0=0, \tag{15}$$

$$Q_2\frac{\partial^2}{\partial T_0^2}\theta_{B0}+Q_9\bar{y}_0+Q_{10}\theta_{B0}+Q_{11}\bar{u}_0+Q_{12}\theta_{A0}=0, \tag{16}$$

$$R_3\frac{\partial^2}{\partial T_0^2}\bar{u}_0+R_9\bar{y}_0+R_{10}\theta_{B0}+R_{11}\bar{u}_0=0, \tag{17}$$

$$S_4\frac{\partial^2}{\partial T_0^2}\theta_{A0}+S_{10}\theta_{B0}+S_{12}\theta_{A0}=0. \tag{18}$$

Equations containing ε^1:

$$\begin{aligned}
&P_1\frac{\partial^2}{\partial T_0^2}\bar{y}_1+P_9\bar{y}_1+P_{10}\theta_{B1}+P_{11}\bar{u}_1\\
&\quad=-2P_1\frac{\partial^2\bar{y}_0}{\partial T_0\partial T_1}-P_5\frac{\partial\bar{y}_0}{\partial T_{01}}-2P_6\frac{\partial\theta_{B0}}{\partial T_0}+P_6\frac{\partial\theta_{B0}}{\partial T_0}\theta_{B0}^2-P_{13}\bar{y}_0\theta_{B0}\bar{u}_0-P_{14}\theta_{B0}\\
&\qquad-P_{15}\bar{u}_0-P_{16}\bar{y}_0^2\theta_{B0}-P_{17}\theta_{B0}\bar{u}_0^2-P_{18}\bar{y}_0^2\bar{u}_0-P_{19}\theta_{B0}^2\bar{u}_0-P_{20}\bar{y}_0\bar{u}_0^2-P_{21}\bar{y}_0^3\\
&\qquad-P_{24}\theta_{B0}^3-P_{26}\bar{u}_0^3-P_{27}\bar{y}_0\theta_{B0}^2+\bar{f}_y,
\end{aligned} \tag{19}$$

$$\begin{aligned}
&Q_2\frac{\partial^2}{\partial T_0^2}\theta_{B1}+Q_9\bar{y}_1+Q_{10}\theta_{B1}+Q_{11}\bar{u}_1+Q_{12}\theta_{A1}\\
&\quad=-2Q_2\frac{\partial^2\theta_{B0}}{\partial T_0\partial T_1}-Q_5\frac{\partial\bar{y}_0}{\partial T_0}+\frac{Q_5}{2}\frac{\partial\theta_{B0}}{\partial T_0}\theta_{B0}^2-Q_6\frac{\partial\theta_{B0}}{\partial T_0}+Q_6\theta_{B0}^2\frac{\partial\theta_{B0}}{\partial T_0}\\
&\qquad-Q_{13}\bar{y}_0\theta_{B0}\bar{u}_0-Q_{16}\bar{y}_0^2\theta_{B0}-Q_{17}\theta_{B0}\bar{u}_0^2-Q_{18}\bar{y}_0^2\bar{u}_0-Q_{19}\theta_{B0}^2\bar{u}_0\\
&\qquad-Q_{20}\bar{y}_0\bar{u}_0^2-Q_{21}\bar{y}_0^3-Q_{24}\theta_{B0}^3-Q_{26}\bar{u}_0^3-Q_{27}\bar{y}_0\theta_{B0}^2-Q_{28}\theta_{A0}^2\theta_{B0}\\
&\qquad-Q_{29}\theta_{B0}^2\theta_{A0}-Q_{30}\theta_{A0}^3+\bar{M}_{\theta_B},
\end{aligned} \tag{20}$$

$$\begin{aligned}
&R_3\frac{\partial^2}{\partial T_0^2}\bar{u}_1+R_9\bar{y}_1+R_{10}\theta_{B1}+R_{11}\bar{u}_1\\
&\quad=-2R_3\frac{\partial^2\bar{u}_0}{\partial T_0\partial T_1}-R_{13}\bar{y}_0\theta_{B0}\bar{u}_0-R_{16}\bar{y}_0^2\theta_{B0}-R_{18}\bar{y}_0^2\bar{u}_0-R_{17}\theta_{B0}\bar{u}_0^2\\
&\qquad-R_{19}\theta_{B0}^2\bar{u}_0-R_{20}\bar{y}_0\bar{u}_0^2-R_{21}\bar{y}_0^3-R_{24}\theta_{B0}^3-R_{26}\bar{u}_0^3-R_{27}\bar{y}_0\theta_{B0}^2\\
&\qquad-R_{31}\theta_{A0}\frac{\partial^2\theta_{A0}}{\partial T_0^2}-R_{33}\left(\frac{\partial\theta_{A0}}{\partial T_0}\right)^2,
\end{aligned} \tag{21}$$

$$\begin{aligned}
&S_4\frac{\partial^2}{\partial T_0^2}\theta_{A1}+S_{10}\theta_{B1}+S_{12}\theta_{A1}\\
&\quad=-2S_4\frac{\partial^2\theta_{A0}}{\partial T_0\partial T_1}-S_{24}\theta_{B0}^3-S_{28}\theta_{B0}\theta_{A0}^2-S_{29}\theta_{A0}\theta_{B0}^2-S_{30}\theta_{A0}^3\\
&\qquad-S_{35}\frac{\partial^2\bar{u}_0}{\partial T_0^2}\theta_{A0}.
\end{aligned} \tag{22}$$

Using Eqs. (15)–(18), the general solutions containing the ε^0 scale can be written as:

$$\begin{aligned}
\bar{y}_0=&A_1V_{11}e^{i\omega_1T_0}e^{-i\beta_1}+A_2V_{12}e^{i\omega_2T_0}e^{-i\beta_2}+A_3V_{13}e^{i\omega_3T_0}e^{-i\beta_3}\\
&+A_4V_{14}e^{i\omega_4T_0}e^{-i\beta_4}+\text{c.c.},
\end{aligned} \tag{23}$$

$$\theta_{B0} = A_1 V_{21} e^{i\omega_1 T_0} e^{-i\beta_1} + A_2 V_{22} e^{i\omega_2 T_0} e^{-i\beta_2} + A_3 V_{23} e^{i\omega_3 T_0} e^{-i\beta_3} + A_4 V_{24} e^{i\omega_4 T_0} e^{-i\beta_4} + \text{c.c.}, \tag{24}$$

$$\bar{u}_0 = A_1 V_{31} e^{i\omega_1 T_0} e^{-i\beta_1} + A_2 V_{32} e^{i\omega_2 T_0} e^{-i\beta_2} + A_3 V_{33} e^{i\omega_3 T_0} e^{-i\beta_3} + A_4 V_{34} e^{i\omega_4 T_0} e^{-i\beta_4} + \text{c.c.}, \tag{25}$$

$$\theta_{A0} = A_1 V_{41} e^{i\omega_1 T_0} e^{-i\beta_1} + A_2 V_{42} e^{i\omega_2 T_0} e^{-i\beta_2} + A_3 V_{43} e^{i\omega_3 T_0} e^{-i\beta_3} + A_4 V_{44} e^{i\omega_4 T_0} e^{-i\beta_4} + \text{c.c.}, \tag{26}$$

where A_n denotes the amplitude; V_{ij} represents the eigenvectors of the system; β_n is the phase angle and c.c. indicates the complex conjugate.

3.2. *Conditions of internal resonance*

In this study, a PTMD is utilized to prevent internal resonance in the main body and reduce vibrations. The concern here is to identify the conditions that cause internal resonance in the main system. First, we consider the equation of motion for vibration in the main body. Using MOMS, we divide the equations of motion for the main body without PTMD (Eqs. (13) and (14)) into two time scales.

Equations containing ε^0:

$$P_1 \frac{\partial^2}{\partial T_0^2} \bar{y}_0 + P_9 \bar{y}_0 + P_{10} \theta_{B0} = 0, \tag{27}$$

$$Q_2 \frac{\partial^2}{\partial T_0^2} \theta_{B0} + Q_9 \bar{y}_0 + Q_{10} \theta_{B0} = 0. \tag{28}$$

Equations containing ε^1:

$$P_1 \frac{\partial^2}{\partial T_0^2} \bar{y}_1 + P_9 \bar{y}_1 + P_{10} \theta_{B1} = \bar{f}_y - 2P_1 \frac{\partial^2 \bar{y}_0}{\partial T_0 \partial T_1} - P_5 \frac{\partial \bar{y}_0}{\partial T_{01}} - 2P_6 \frac{\partial \theta_{B0}}{\partial T_0} + P_6 \frac{\partial \theta_{B0}}{\partial T_0} \theta_{B00}^2 - P_{14} \theta_{B0} - P_{16} \bar{y}_0^2 \theta_{B0} - P_{21} \bar{y}_0^3 - P_{24} \theta_{B0}^3 - P_{27} \bar{y}_0 \theta_{B0}^2, \tag{29}$$

$$Q_2 \frac{\partial^2 \theta_{B1}}{\partial T_0^2} + Q_9 \bar{y}_1 + Q_{10} \theta_{B1} = \bar{M}_{\theta_B} - 2Q_2 \frac{\partial^2 \theta_{B0}}{\partial T_0 \partial T_1} - Q_5 \frac{\partial \bar{y}_0}{\partial T_0} + \frac{Q_5}{2} \frac{\partial \theta_{B0}}{\partial T_0} \theta_{B0}^2 - Q_6 \frac{\partial \theta_{B0}}{\partial T_0} + Q_6 \theta_{B0}^2 \frac{\partial \theta_{B0}}{\partial T_0} - Q_{16} \bar{y}_0^2 \theta_{B0} - Q_{21} \bar{y}_0^3 - Q_{24} \theta_{B0}^3 - Q_{27} \bar{y}_0 \theta_{B0}^2. \tag{30}$$

The coefficients in Eqs. (27)–(30) are presented in letters, the details of which are presented in Appendix C. Equations (27) and (28) are rewritten in matrix form as follows:

$$\begin{bmatrix} 1 & 0 \\ 0 & 1 \end{bmatrix} \begin{Bmatrix} \partial^2 \bar{y}_0 / \partial \tau^2 \\ \partial^2 \theta_{B0} / \partial \tau^2 \end{Bmatrix} + \begin{bmatrix} 1 & (\bar{l}_1 - \bar{l}_2)/2 \\ \bar{\omega}_{\theta_B}^2 (\bar{l}_1 - \bar{l}_2) & \bar{\omega}_{\theta_B}^2 (\bar{l}_1^2 - \bar{l}_2^2) \end{bmatrix} \begin{Bmatrix} \bar{y}_0 \\ \theta_{B0} \end{Bmatrix} = \begin{Bmatrix} 0 \\ 0 \end{Bmatrix}.$$

Clearly, the solution can be considered as a simple harmonic motion, for which it is assumed $\bar{y}_0 = \tilde{\bar{y}}_0 e^{i\omega\tau}$, $\theta_{B0} = \tilde{\theta}_{B0} e^{i\omega\tau}$, where ω is the natural frequency. The associated eigen-equation is:

$$e^{i\omega\tau}\begin{bmatrix} -\omega^2+1 & \dfrac{(\bar{l}_1-\bar{l}_2)}{2} \\ \bar{\omega}^2_{\theta_B}(\bar{l}_1-\bar{l}_2) & -\omega^2+\bar{\omega}^2_{\theta_B}(\bar{l}_1^2+\bar{l}_2^2) \end{bmatrix}\begin{Bmatrix} \tilde{\bar{y}} \\ \tilde{\theta}_B \end{Bmatrix} = \begin{Bmatrix} 0 \\ 0 \end{Bmatrix}.$$

Let $\lambda = \omega^2$ in which λ is the eigenvalue, we can derive that

$$\lambda_1 = \frac{1}{2}+\frac{1}{2}\bar{\omega}^2_{\theta_B}(\bar{l}_1^2+\bar{l}_2^2) - \frac{1}{2}\sqrt{1+\bar{\omega}^4_{\theta_B}(\bar{l}_1^4+2\bar{l}_1^2\bar{l}_2^2+\bar{l}_2^4)-4\bar{\omega}^2_{\theta_B}\bar{l}_1\bar{l}_2},$$

$$\lambda_2 = \frac{1}{2}+\frac{1}{2}\bar{\omega}^2_{\theta_B}(\bar{l}_1^2+\bar{l}_2^2) + \frac{1}{2}\sqrt{1+\bar{\omega}^4_{\theta_B}(\bar{l}_1^4+2\bar{l}_1^2\bar{l}_2^2+\bar{l}_2^4)-4\bar{\omega}^2_{\theta_B}\bar{l}_1\bar{l}_2},$$

where $I_B = (Ml^2/12) + M((l/2)-l_1)^2$ and $\bar{\omega}^2_{\theta_B} = (Kl^2/I_B)/(2K/M) = 3/(2-6\bar{l}_1+6\bar{l}_1^2)$. Supposing that $\bar{l}=1$, then $\bar{l}_2 = 1-\bar{l}_1$. The simplified eigenvalues are thus

$$\frac{1}{2}+\frac{3(\bar{l}_1^2+\bar{l}_2^2)}{4-12\bar{l}_1+12\bar{l}_1^2} - \frac{1}{2}\sqrt{1+\frac{9(\bar{l}_1^4+2\bar{l}_1^2\bar{l}_2^2+\bar{l}_2^4)}{(2-6\bar{l}_1+6\bar{l}_1^2)^2}-\frac{6\bar{l}_1\bar{l}_2}{1-3\bar{l}_1+3\bar{l}_1^2}} \quad \text{and}$$

$$\frac{1}{2}+\frac{3(\bar{l}_1^2+\bar{l}_2^2)}{4-12\bar{l}_1+12\bar{l}_1^2} + \frac{1}{2}\sqrt{1+\frac{9(\bar{l}_1^4+2\bar{l}_1^2\bar{l}_2^2+\bar{l}_2^4)}{(2-6\bar{l}_1+6\bar{l}_1^2)^2}-\frac{6\bar{l}_1\bar{l}_2}{1-3\bar{l}_1+3\bar{l}_1^2}}.$$

For the condition $0 < \bar{l}_1 < 1$, the following typical cases are considered:

(a) If the ratio of the two eigenvalues is 1:1, then $\bar{l}_1$ cannot satisfy the aforementioned conditions.
(b) If the ratio of the two eigenvalues is 1:4, then $\bar{l}_1 = 0.17837$ or 0.82163.
(c) If the ratio of the two eigenvalues is 1:9, then $\bar{l}_1 = 1.1565$ or -0.15646 and therefore does not satisfy the aforementioned conditions either.

In the above discussion, it is found that the 1:2 internal resonance ($\omega_y : \omega_{\theta_B} = 1:2$ or $\lambda_1 : \lambda_2 = 1:4$) may occur at $\bar{l}_1 = 0.17837$ or 0.82163.

3.3. *Frequency response*

Using the MOMS, we divide the equations of motion (Eqs. (9)–(12)) in the system into equations comprising ε^0 terms (Eqs. (15)–(18)) and ε^1 terms (Eqs. (19)–(22)), of which the set of equations comprising ε^0 terms can be written as:

$$\mathbf{A}\frac{\partial^2 \mathbf{X}_0}{\partial \tau^2} + \mathbf{B}\mathbf{X}_0 = 0,$$

in which

$$\mathbf{A} = \begin{bmatrix} P_1 & P_2 & P_3 & P_4 \\ Q_1 & Q_2 & Q_3 & Q_4 \\ R_1 & R_2 & R_3 & R_4 \\ S_1 & S_2 & S_3 & S_4 \end{bmatrix}, \quad \mathbf{B} = \begin{bmatrix} P_9 & P_{10} & P_{11} & P_{12} \\ Q_9 & Q_{10} & Q_{11} & Q_{12} \\ R_9 & R_{10} & R_{11} & R_{12} \\ S_9 & S_{10} & S_{11} & S_{12} \end{bmatrix} \quad \text{and}$$

$$\mathbf{X}^T = [\, y_0 \quad \theta_{B0} \quad u_0 \quad \theta_{A0} \,].$$

The equations comprising ε^1 terms can also be written as:

$$\mathbf{A}\frac{\partial^2 \mathbf{X}_1}{\partial \tau^2} + \mathbf{B}\mathbf{X}_1 = \mathbf{F}.$$

We multiply both of these equations by the inverse ($\mathbf{V}^{-1}$) of the eigenvector ($\mathbf{V}$) in the system, in which $\mathbf{X}_1 = \mathbf{V}\mathbf{Y}$,

$$\mathbf{V} = \begin{bmatrix} V_{11} & V_{12} & V_{13} & V_{14} \\ V_{21} & V_{22} & V_{23} & V_{24} \\ V_{31} & V_{32} & V_{33} & V_{34} \\ V_{41} & V_{42} & V_{43} & V_{44} \end{bmatrix}, \quad \mathbf{Y}^T = [\, \bar{y}_1 \quad \theta_{B1} \quad \bar{u} \quad \theta_{A1} \,] \quad \text{and}$$

$$\mathbf{F}^T = [\, F_1 \quad F_2 \quad F_3 \quad F_4 \,].$$

Based on the orthogonality of the eigenvector, we can decouple ε^1 equations and rewrite them as:

$$\begin{bmatrix} 1 & 0 & 0 & 0 \\ 0 & 1 & 0 & 0 \\ 0 & 0 & 1 & 0 \\ 0 & 0 & 0 & 1 \end{bmatrix} \begin{Bmatrix} \partial^2 \bar{y}_1/\partial\tau^2 \\ \partial^2 \theta_{B1}/\partial\tau^2 \\ \partial^2 \bar{u}_1/\partial\tau^2 \\ \partial^2 \theta_{A1}/\partial\tau^2 \end{Bmatrix} + \begin{bmatrix} \omega_1^2 & 0 & 0 & 0 \\ 0 & \omega_2^2 & 0 & 0 \\ 0 & 0 & \omega_3^2 & 0 \\ 0 & 0 & 0 & \omega_4^2 \end{bmatrix} \begin{Bmatrix} \bar{y}_1 \\ \theta_{B1} \\ \bar{u}_1 \\ \theta_{A1} \end{Bmatrix} = \begin{Bmatrix} \bar{\Gamma}_1 \\ \bar{\Gamma}_2 \\ \bar{\Gamma}_3 \\ \bar{\Gamma}_4 \end{Bmatrix}, \tag{31}$$

where

$$\bar{\Gamma}_n = \mathbf{V}^{-1}\mathbf{A}^{-1}\mathbf{F}_n, \quad n = 1 \sim 4. \tag{32}$$

$$\begin{aligned} F_1 = {} & \bar{f}_y - 2P_1\frac{\partial^2 \bar{y}_0}{\partial T_0 \partial T_1} - P_5\frac{\partial \bar{y}_0}{\partial T_{01}} - 2P_6\frac{\partial \theta_{B0}}{\partial T_0} + P_6\frac{\partial \theta_{B0}}{\partial T_0}\theta_{B00}^2 - P_{13}\bar{y}_0\theta_{B0}\bar{u}_0 \\ & - P_{14}\theta_{B0} - P_{15}\bar{u}_0 - P_{16}\bar{y}_0^2\theta_{B0} - P_{17}\theta_{B0}\bar{u}_0^2 - P_{18}\bar{y}_0^2\bar{u}_0 - P_{19}\theta_{B0}^2\bar{u}_0 \\ & - P_{20}\bar{y}_0\bar{u}_0^2 - P_{21}\bar{y}_0^3 - P_{24}\theta_{B0}^3 - P_{26}\bar{u}_0^3 - P_{27}\bar{y}_0\theta_{B0}^2, \end{aligned} \tag{33}$$

$$\begin{aligned} F_2 = {} & \bar{M}_{\theta_B} - 2Q_2\frac{\partial^2 \theta_{B0}}{\partial T_0 \partial T_1} - Q_5\frac{\partial \bar{y}_0}{\partial T_0} + \frac{Q_5}{2}\frac{\partial \theta_{B0}}{\partial T_0}\theta_{B0}^2 - Q_6\frac{\partial \theta_{B0}}{\partial T_0} + Q_6\theta_{B0}^2\frac{\partial \theta_{B0}}{\partial T_0} \\ & - Q_{19}\bar{u}_0\theta_{B0}^2 - Q_{24}\theta_{B0}^3 - Q_{27}\bar{y}_0\theta_{B0}^2 - Q_{28}\theta_{A0}^2\theta_{B0} - Q_{29}\theta_{B0}^2\theta_{A0} - Q_{30}\theta_{A0}^3, \end{aligned} \tag{34}$$

$$F_3 = -2R_3\frac{\partial^2}{\partial T_0 \partial T_1}\bar{u}_0 - R_{13}\bar{y}_0\theta_{B0}\bar{u}_0 - R_{16}\bar{y}_0^2\theta_{B0} - R_{18}\bar{y}_0^2\bar{u}_0 - R_{17}\theta_{B0}\bar{u}_0^2$$
$$- R_{19}\theta_{B0}^2\bar{u}_0 - R_{20}\bar{y}_0\bar{u}_0^2 - R_{21}\bar{y}_0^3 - R_{24}\theta_{B0}^3 - R_{26}\bar{u}_0^3 - R_{27}\bar{y}_0\theta_{B0}^2$$
$$- R_{31}\theta_{A0}\frac{\partial^2\theta_{A0}}{\partial T_0^2} - R_{33}\left(\frac{\partial\theta_{A0}}{\partial T_0}\right)^2, \tag{35}$$

$$F_4 = -2S_4\frac{\partial^2\theta_{A0}}{\partial T_0 \partial T_1} - S_{24}\theta_{B0}^3 - S_{28}\theta_{B0}\theta_{A0}^2 - S_{29}\theta_{A0}\theta_{B0}^2 - S_{30}\theta_{A0}^3$$
$$- S_{35}\frac{\partial^2\bar{u}_0}{\partial T_0^2}\theta_{A0}. \tag{36}$$

To observe the influence of external excitation on different DOFs, we hypothesize that the external force term is

$$\bar{f} = \hat{f}e^{i\Omega T_0} = \hat{f}e^{i(\omega_i+\varepsilon\sigma)T_0} = \hat{f}e^{i\omega_i T_0}e^{i\sigma\varepsilon T_0} = \hat{f}e^{i\omega_i\tau}e^{i\sigma T_1}. \tag{37}$$

By respectively substituting Eqs. (33)–(36) into Eq. (32), we can obtain $\bar{\Gamma}_n$, which, when successively substituted into Eq. (31), gives us the secular terms for the DOF in question. It is worth mentioning that the so-called secular terms (divisor terms) in MOMS refer to the terms on the right side of the dynamic equation (Eq. (31)). If this frequency is equal to the natural frequency of the system on the left-hand side of the equation, then the system will have no convergent solutions, which are secular terms. We thus select all of the harmonic terms on the right-hand side of the equation with the same frequency as the natural frequency of the system and assume that the equations comprising the secular terms are 0, which enable us to derive the solvability conditions. The σ in Eq. (37) is the detuned frequency. We then plot a frequency response graph with σ as the horizontal axis and amplitude as the vertical axis so as to observe the changes in amplitude in the DOF near the resonance frequency. Take, for example, the excitation of the first and second DOFs when the main body is equipped with the PTMD. When the first DOF (y-DOF) is excited, $\bar{f} = \hat{f}e^{i\Omega\tau} = \hat{f}e^{i\sigma_1 T_1}e^{i\omega_1 T_0}$, where σ_1 represents detuned frequency for exciting the first DOF. To facilitate the solution process and obtain the steady-state response solution, we set

$$\frac{\partial A_1}{\partial T_1} = 0 \quad \text{and} \quad \frac{\partial A_2}{\partial T_1} = 0.$$

When the first DOF (y-DOF) is excited, we can derive the relationship between σ_1 and the amplitudes of the excited DOFs from the solvability conditions, whereby we can draw a Fixed Points plots. Furthermore, it is worth noting that the internal resonance frequency previously found for the main body is $\omega_1 : \omega_2 = 1:2$. If the natural vibration frequency of this DOF equals ω_1, then the frequencies capable of inducing resonance include $\omega_2 - \omega_1$ in addition to ω_1. In other words, the secular

terms under these circumstances must include the terms $e^{i\omega_1 T_0}$ and $e^{i(\omega_2-\omega_1)T_0}$ on the right-hand side of Eq. (31).

If the second mode is excited ($\bar{f} = \hat{f}e^{i\Omega\tau} = \hat{f}e^{i\sigma_2 T_1}e^{i\omega_2 T_0}$), where σ_2 represents the detuned frequency for the second DOF, we can also use the above approach to obtain the solvability conditions. Again, with the previously determined internal resonance frequency of $\omega_1 : \omega_2 = 1:2$, if the natural vibration frequency of the DOF is ω_2, then when the second mode is being excited, the frequencies including ω_2 as $2\omega_1$ may induce resonance.

4. Results and Discussion

This study examines the effect of vibration reduction of the mass ratio ($\bar{m}$), location, extension spring constant ($\hat{k}_S$) and torsion spring constant ($\hat{k}_T$) of the PTMD installed on a slender rigid body with 1:2 internal resonance. For a nonlinear system, a number of parameters exist, for which we shall use the concept of an IRCP[8] and 3D graphics to identify circumstances capable of preventing internal resonance. Under such circumstances, we then derive the best combination of parameters that is capable of inhibiting vibration in the main body.

In particular, a 3D-IRCP aided by various amplitude analysis tables is proposed in this study for the identification of PTMD parameter combinations capable of preventing internal resonance. This approach enables designers to evaluate the effectiveness of various parameter combinations of the PTMD prior to the design process. Due to the complicated nature of coupled nonlinear torsion-extension spring of the PTMD, the experimental and analytical procedures in finding the optimal combination of the PTMD parameters are beyond the present discussion.

4.1. *Internal resonance analysis*

We first confirm whether internal resonance exists in the main body, for which the frequency responses of the main body under force without a PTMD are discussed. Figures 2 and 3 respectively display the fixed points plots of the first and second DOFs when the first DOF is under excitation by a force applied at $X_F = 0.3\bar{l}$ from the center of mass of the main body. Furthermore, we include six small graphs showing the time domain responses and Poincaré maps corresponding to various frequencies for the confirmation of mutual accuracy. A comparison of the fixed-point plots in Figs. 2 and 3 reveals that the amplitudes of the first DOF are greater than those of the second DOF, which is normal in excitation. From Fig. 2, $\sigma = 4$, we can clearly observe the jump phenomenon, which refers to a structurally adverse condition in which a frequency corresponds to two or more amplitudes, creating instability in the particular areas of the system. Time domain responses corresponding to $\sigma = 4$ and the chaos phenomena displayed in the Poincaré maps also present characteristics of instability. Furthermore, the Poincaré maps corresponding to $\sigma = 0$ and -10 are the L.C.O. (limit cycle oscillations).

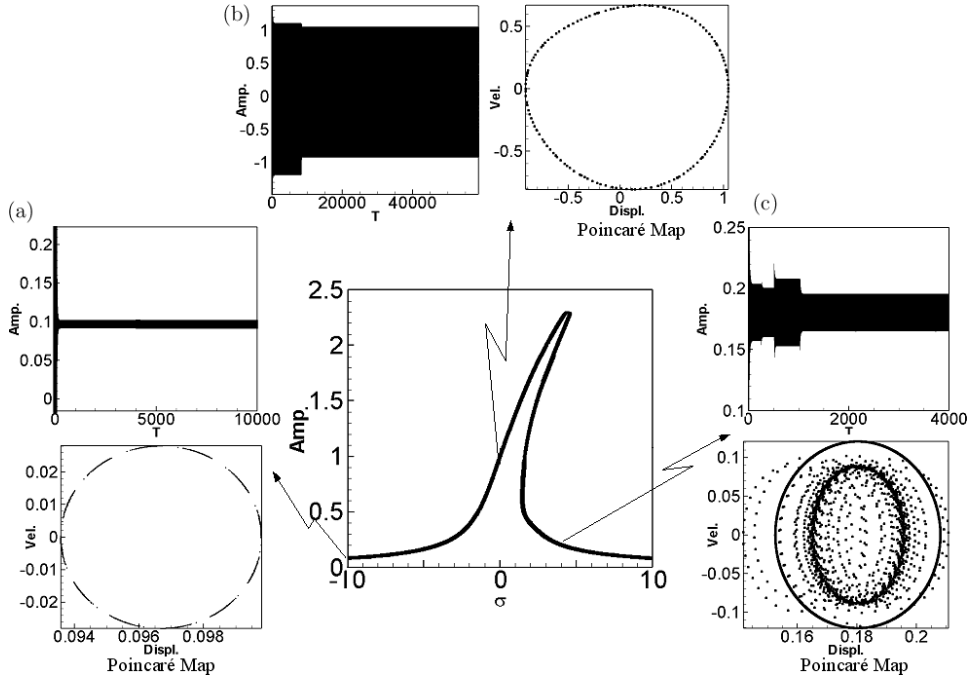

Fig. 2. No PTMD, first mode fixed points plots, $X_F = 0.3\bar{l}$, excite first DOF. (a) $\sigma = -10.0$; (b) $\sigma = 0.0$; (c) $\sigma = 4.0$.

Figures 4 and 5 respectively show the fixed points plots of the first and second DOFs when the second DOF is being excited by a force applied at $X_F = 0.3\bar{l}$ from the center of mass of the main body. A comparison of the fixed-point plots in Figs. 4 and 5 indicates that the amplitudes of the first DOF are also greater than those of the second DOF, which is an internal resonance phenomenon unique to nonlinear systems. This confirms the existence of internal resonance in the main body.

In Fig. 4, an unstable region is formed when $\sigma = 3$. The time domain responses and Poincaré maps also clearly display characteristics of instability.

4.2. *Vibration analysis of system with PTMD*

Due to the existence of internal resonance and vibration characteristics in the main body, we add a PTMD capable of swinging and moving in the transverse direction to prevent internal resonance, while inhibiting vibrations. The purposes of the PTMD are as follows: (1) to prevent internal resonance, (2) to identify the location for the PTMD to effectively reduce vibration, and (3) to determine the influence of parameters including the mass ratio ($\bar{m}$) of the PTMD, the suspension location of the PTMD, the dimensionless extension spring constant ($\hat{k}_S$), and the dimensionless torsion spring constant ($\hat{k}_T$).

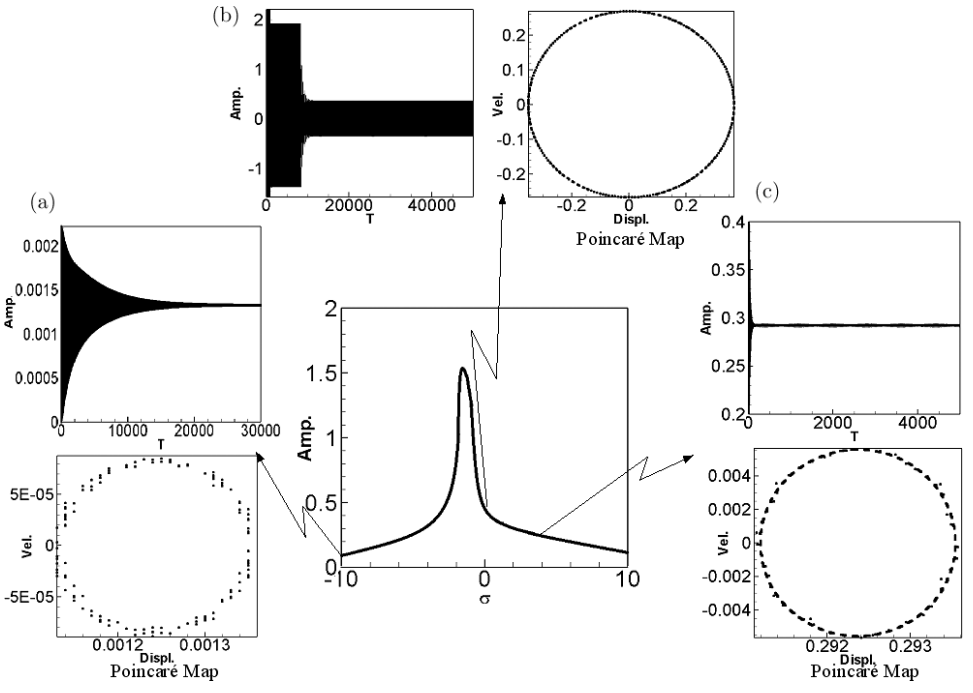

Fig. 3. No PTMD, second mode fixed points plots, $X_F = 0.3\bar{l}$, excite first DOF. (a) $\sigma = -10.0$; (b) $\sigma = 0.0$; (c) $\sigma = 4.0$.

4.2.1. *Prevention of internal resonance*

Figure 6 shows a 3D-IRCP that considers four variables for preventing internal resonance: the mass ratio ($\bar{m}$), the location of the PTMD, the extension spring constant ($\hat{k}_S$) and the torsion spring constant ($\hat{k}_T$). Frequency differences of less than 0.1% in the various combinations (meaning that there is a high chance of internal resonance) are displayed using symbols. The X, Y and Z axes respectively denote the dimensionless torsion spring constant ($\hat{k}_T$), dimensionless extension spring constant ($\hat{k}_S$) and location of the PTMD. The mass ratio ($\bar{m}$) of the PTMD is presented using various shapes and colors. We call this 3D graph of internal resonance occurring with various combinations the 3D-IRCP, which reveals the capacity of various combinations to prevent internal resonance and reminds designers of the combinations to avoid, thereby maximizing the effectiveness of the PTMD. To facilitate discussion, we divide Fig. 6 into two sections ($0.09 \leq \bar{m} \leq 0.25$ and $0.3 \leq \bar{m} \leq 0.5$). An observation of Fig. 6 shows that the majority of the $\hat{k}_T$ variations appear in horizontal lines (fixed values); therefore, we need to consider only the relationships among $\bar{m}$, $\hat{k}_S$, and the location of the PTMD. Figure 7 shows the 2D-IRCP of Fig. 6 for $0.09 \leq \bar{m} \leq 0.25$, projecting various $\hat{k}_T$ values onto the $\hat{k}_S$ and PTMD location plane. By comparison of the green square symbols ($\bar{m} = 0.1$) and the yellow circle symbols ($\bar{m} = 0.25$), we find that within the range of $0.1 \leq \bar{m} \leq 0.25$, the range of $\hat{k}_S$

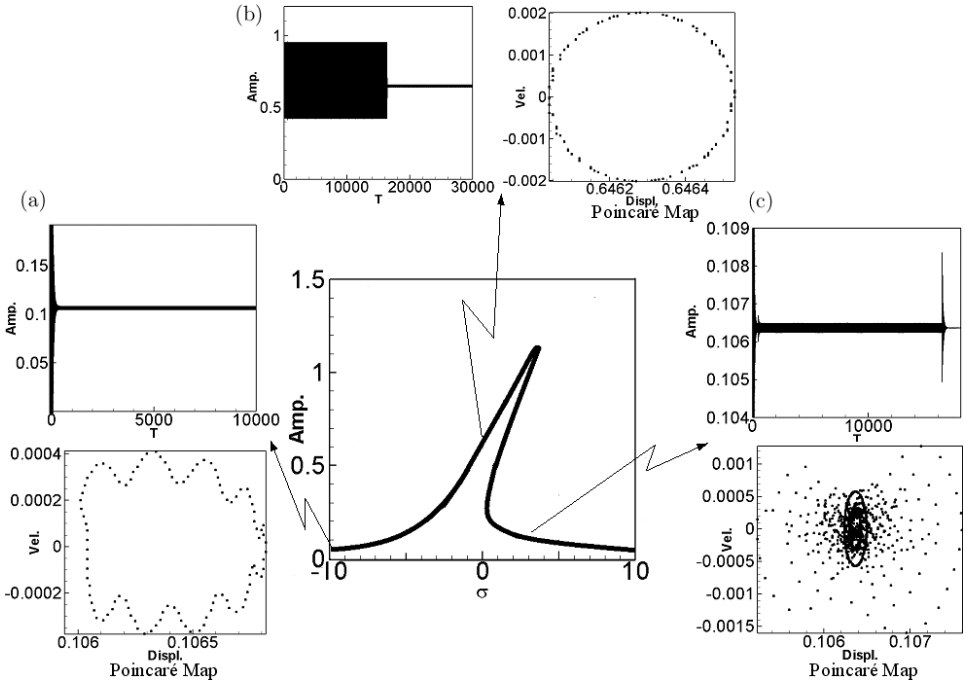

Fig. 4. No PTMD, first mode fixed points plots, $X_F = 0.3\bar{l}$, excite second DOF. (a) $\sigma = -10.0$; (b) $\sigma = 0.0$; (c) $\sigma = 3.0$.

in which internal resonance may occur increases with $\bar{m}$. In other words, when $\bar{m} = 0.25$, there are more PTMD locations and combinations of $\hat{k}_S$ and $\hat{k}_T$ that will induce internal resonance. The effectiveness in preventing internal resonance is reduced. Therefore, $\bar{m} = 0.25$ should be avoided. Figure 8 shows the 2D-IRCP of Fig. 6 with $0.3 \leq \bar{m} \leq 0.5$, projecting the mass ratios related to various $\hat{k}_T$ values onto the $\hat{k}_S$ and PTMD location plane. In contrast, as $\bar{m}$ increases, we observe a narrowing in the range of PTMD locations and $\hat{k}_S$ in which internal resonance occurs. In other words, within the range of $0.3 \leq \bar{m} \leq 0.5$, either a smaller mass ratio ($\bar{m} = 0.3$) shows a smaller range of $\hat{k}_S$ values to prevent internal resonance, or a greater mass ratio ($\bar{m} = 0.5$) shows a greater range of PTMD locations and $\hat{k}_S$ values capable of preventing internal resonance.

To provide a more detailed explanation of the results in Fig. 8 and the effect of the PTMD location in preventing internal resonance, we take $\bar{m} = 0.3$ as an example (Fig. 9). With mass ratios projected onto the $\hat{k}_S$ and PTMD location plane with regard to different $\hat{k}_T$ values, we can see that when $\hat{k}_S = 0.2$, internal resonance can be prevented as long as the distance between the PTMD and the left end of the main body (x_D) is less than $0.6\bar{l}$. Also, when $\hat{k}_S = 0.3$, internal resonance can be prevented as long as x_D is less than $0.4\bar{l}$. This demonstrates that adjusting the location of the PTMD is an effective means of preventing internal resonance. To confirm the

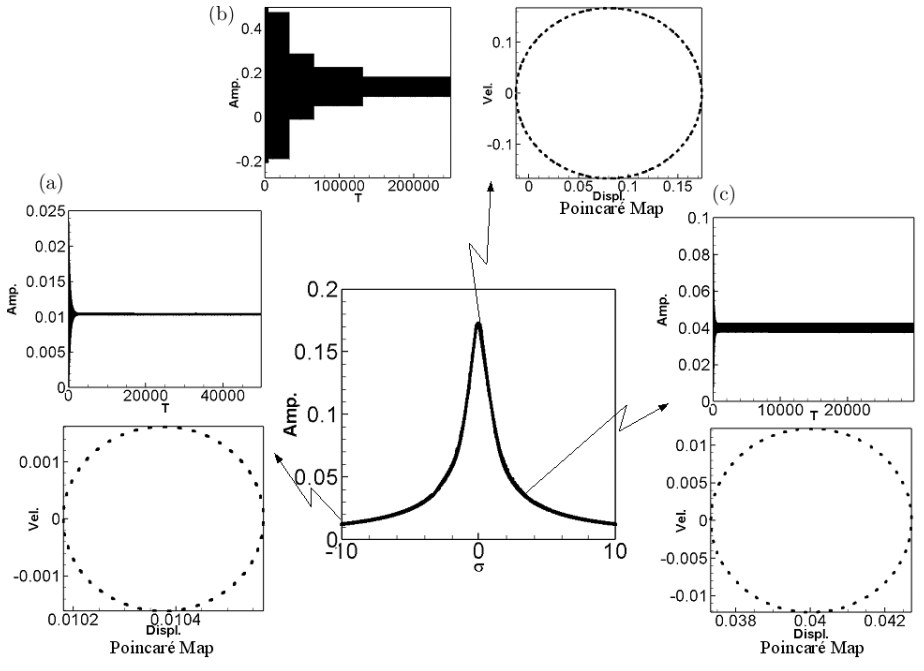

Fig. 5. No PTMD, second mode fixed points plots, $X_F = 0.3\bar{l}$, excite second DOF. (a) $\sigma = -10.0$; (b) $\sigma = 0.0$; (c) $\sigma = 3.0$.

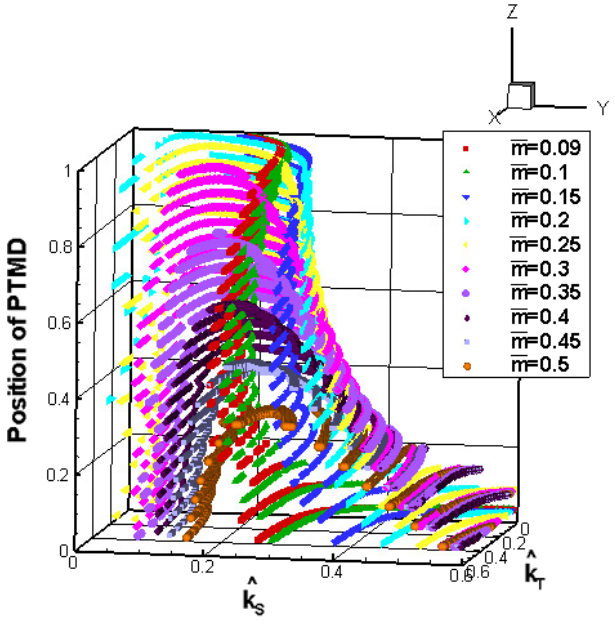

Fig. 6. 3D-IRCP of this system.

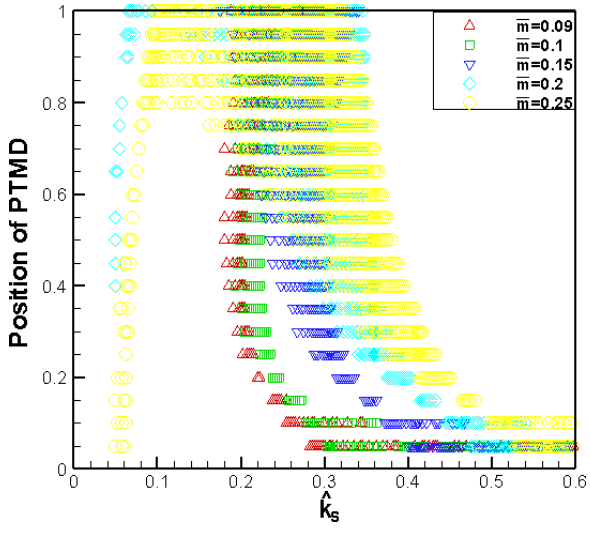

Fig. 7. 2D-IRCP ($0.09 \leq \bar{m} \leq 0.25$).

accuracy of Fig. 9, we select four stricter points in Fig. 9: (0.18, 0.6), (0.2, 0.6), (0.28, 0.4), and (0.3, 0.4). We then employ the fixed points plots in Figs. 10–13, in which the first DOF (y-DOF) and second DOF (θ_B-DOF) are respectively excited to verify the four points in Fig. 9. In Figs. 10–13, $\hat{k}_T$ is fixed at 0.5 and the location of the PTMD is the same. Under these circumstances, slight adjustments to $\hat{k}_S$ are sufficient to prevent internal resonance. We find that internal resonance occurs at (0.2, 0.6) and (0.3, 0.4) in Fig. 9 and in their corresponding points in Figs. 11 and 13.

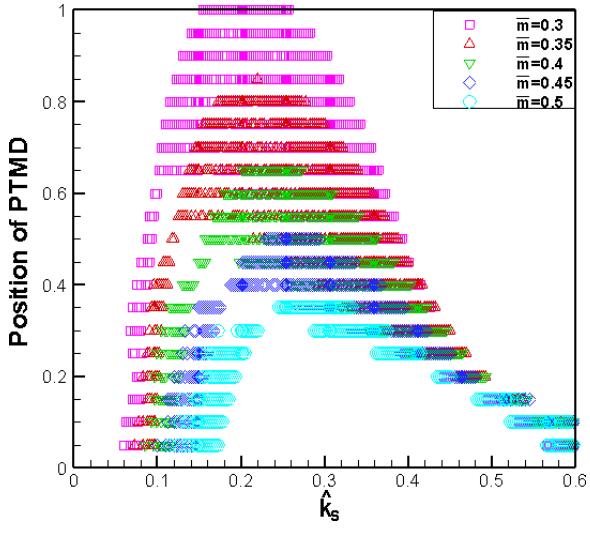

Fig. 8. 2D-IRCP ($0.3 \leq \bar{m} \leq 0.5$).

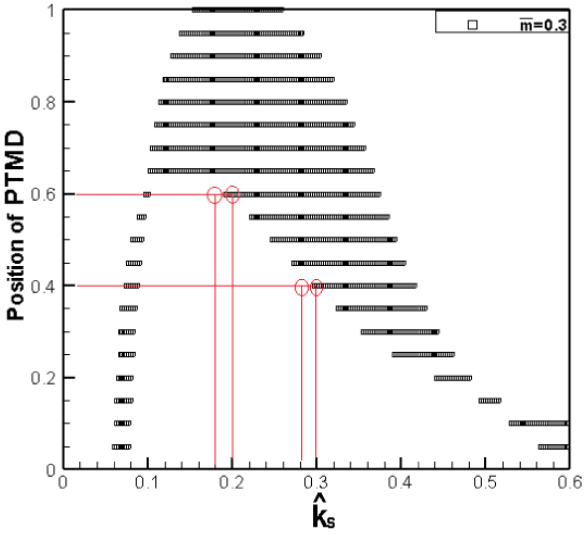

Fig. 9. 2D-IRCP for $\bar{m} = 0.3$.

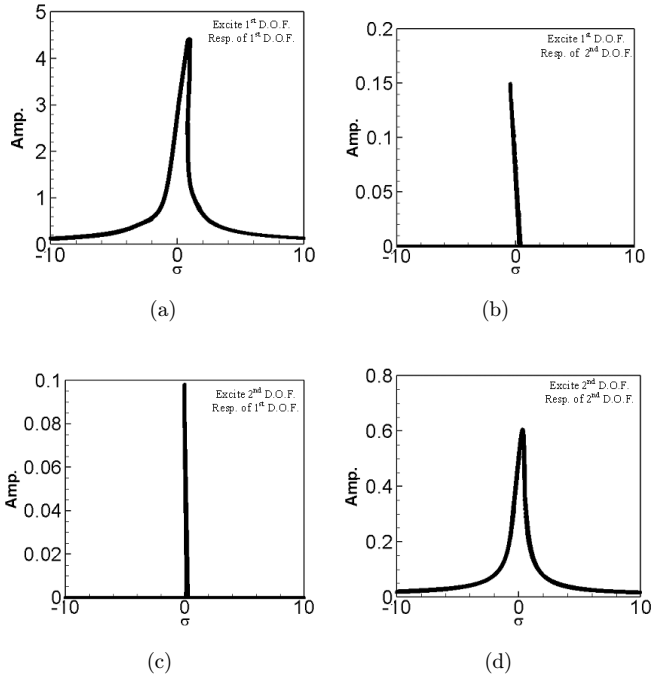

Fig. 10. Fixed point plots of the case $\bar{m} = 0.3$, $\hat{k}_S = 0.18$, position of PTMD = 0.6. (a) Excite first DOF, resp. of first DOF; (b) excite first DOF, resp. of second DOF; (c) excite second DOF, resp. of first DOF; (d) excite second DOF, resp. of second DOF.

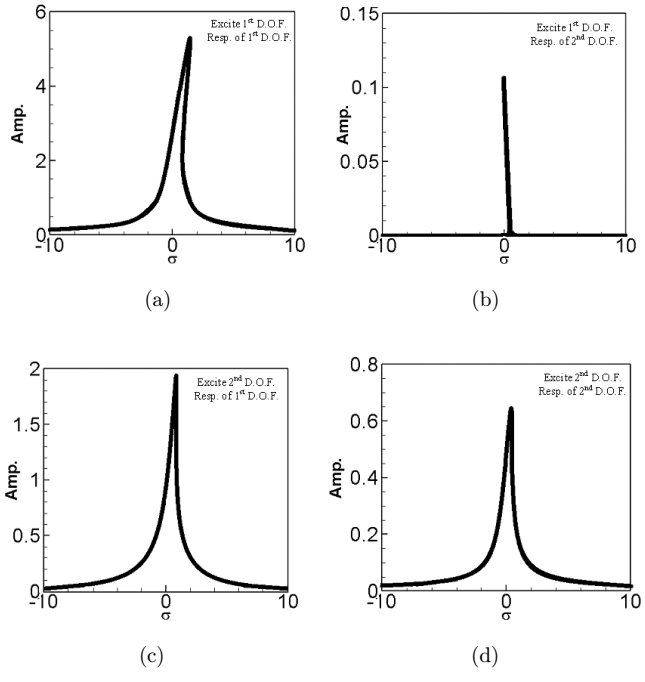

Fig. 11. Fixed point plots of the case $\bar{m} = 0.3$, $\hat{k}_S = 0.2$, position of PTMD = 0.6. (a) Excite first DOF, resp. of first DOF; (b) excite first DOF, resp. of second DOF; (c) excite second DOF, resp. of first DOF; (d) excite second DOF, resp. of second DOF.

Through mutual accuracy confirmation, the reliability of the graphs is enhanced. As previously mentioned, $\hat{k}_T$ rarely changes, for which we first did not consider $\hat{k}_T$ in Figs. 10–13. The influence of $\hat{k}_T$ on the system will be discussed later.

Figures 14 and 15 show the selection bases for $\hat{k}_S$ and $\hat{k}_T$, respectively, projecting four PTMD mass ratios ($\bar{m}$) from the IRCP with varying $\hat{k}_T$ and $\hat{k}_S$ values onto the $\hat{k}_S$, $\hat{k}_T$, and PTMD location planes. To prevent internal resonance, we select the dimensionless spring constant based on these graphs. From the four different $\bar{m}$ values in Fig. 14 and the range of possible internal resonance occurrence ($0.1 \leq \hat{k}_S \leq 0.55$ in Fig. 14), we can still find a "better $\hat{k}_S$" that enables a larger range of PTMD locations to prevent internal resonance. We randomly select a better $\hat{k}_S$ value from $0.1 \leq \hat{k}_S \leq 0.55$ in Fig. 14, indicated with a red arrow. From the four mass ratios ($\bar{m}$) of the PTMD in Fig. 15, we derive a correspondingly better $\hat{k}_T$. It is worth noting that significantly greater or smaller spring constants can prevent internal resonance, but adversely affect damping. If the spring constant is too great, the spring cannot lengthen easily, thereby hindering the movement of the PTMD and limiting its influence. If the spring constant is too small, then the spring can be stretched too easily, resulting in excessive motion of the PTMD, which can destabilize the system. The red arrow in Fig. 15 indicates the better $\hat{k}_T$ (which provides a relatively greater number of PTMD locations to prevent internal resonance). An

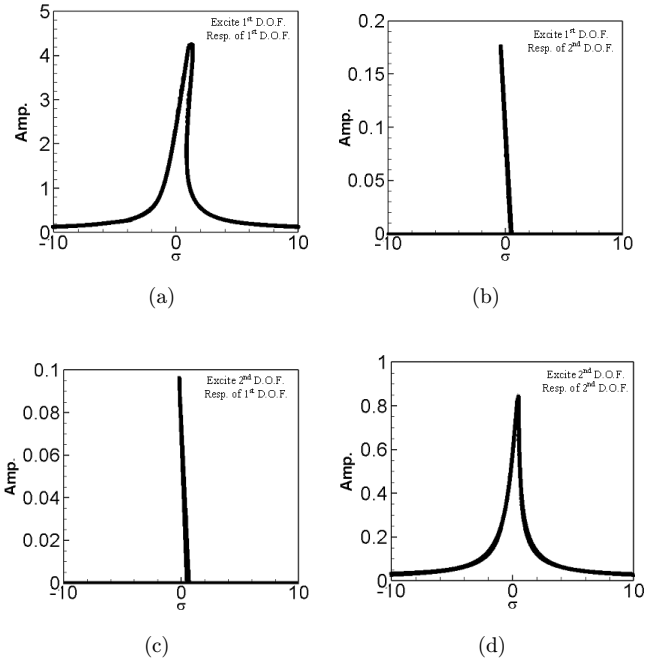

Fig. 12. Fixed point plots of the case $\bar{m} = 0.3$, $\hat{k}_S = 0.28$, position of PTMD = 0.4. (a) Excite first DOF, resp. of first DOF; (b) excite first DOF, resp. of second DOF; (c) excite second DOF, resp. of first DOF; (d) excite second DOF, resp. of second DOF.

observation of Figs. 14 and 15 indicates that under the same $\bar{m}$, changing $\hat{k}_S$ to prevent internal resonance is considerably more effective than changing $\hat{k}_T$. This is the reason why we consider $\bar{m}$ and $\hat{k}_S$ first, in our selection of PTMD parameters. Figure 15 shows that in most circumstances, the probability of internal resonance (black squared locations) does not vary significantly as $\hat{k}_T$ changes. This may be due to the fact that changes in the $\hat{k}_T$ value have limited influence on changes in the overall vibration frequency. For this reason, changing $\hat{k}_T$ is not an effective approach to prevent internal resonance. The discussion above focuses only on the effectiveness of changing spring constants for prevention of internal resonance. The effectiveness of these parameters in vibration reduction will be discussed in later sections (Sec. 4.2.3 and Table 10). It is actually not true that selecting a $\hat{k}_T$ from Fig. 15 will fail to prevent internal resonance in most PTMD locations, regardless of the $\hat{k}_T$ value. We will therefore explain the means of selecting a $\hat{k}_T$ in Fig. 16, which is the IRCP of the PTMD mass ratio combinations with $\bar{m} = 0.09$, 0.1, 0.3, 0.5. From Fig. 15, we can see that when $\bar{m} = 0.09$, a preferable torsion spring constant is $\hat{k}_T = 0.5$. An observation of only Fig. 15 indicates that any PTMD located more than $0.6\bar{l}$ from the left-end body is unable to prevent internal resonance. However, Fig. 16 shows that if we select an appropriate $\hat{k}_S$, such as the combination of $\hat{k}_S = 0.5$ and $\hat{k}_T = 0.5$, then internal resonance can be prevented, regardless of the PTMD

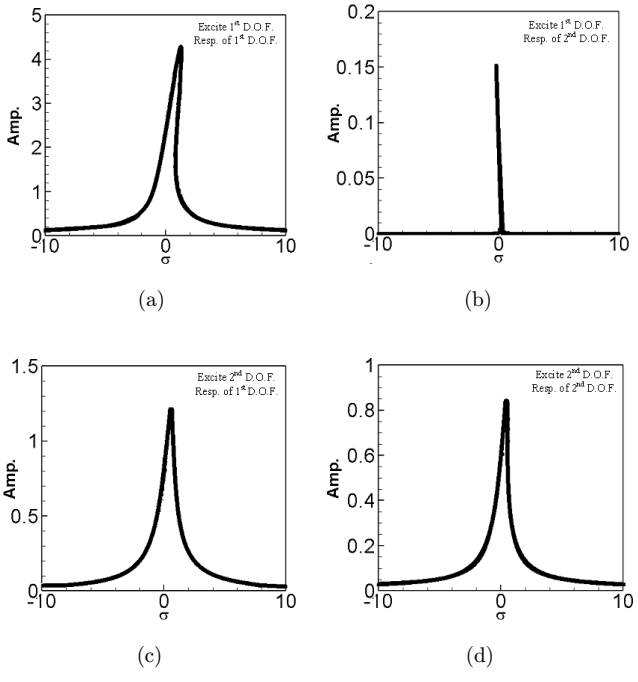

Fig. 13. Fixed point plots of the case $\bar{m} = 0.3$, $\hat{k}_S = 0.3$, position of PTMD = 0.4. (a) Excite first DOF, resp. of first DOF; (b) excite first DOF, resp. of second DOF; (c) excite second DOF, resp. of first DOF; (d) excite second DOF, resp. of second DOF.

location. Similarly, we can derive the principles of selecting $\hat{k}_T$ from other PTMD mass ratios ($\bar{m}$). For instance, when $\bar{m} = 0.1$, the best $\hat{k}_T$ is 0.45; when $\bar{m} = 0.3$, the best $\hat{k}_T$ is 0.1, and when $\bar{m} = 0.5$, the best value of $\hat{k}_T$ is 0.35.

4.2.2. *Influence of PTMD location on amplitude*

We first install the PTMD at various locations to investigate its influence on the vibration of the system. The peak amplitudes of each DOF in the main body are presented in Tables 1–9 (including those without PTMD). We then divide the peak amplitudes by those on the same DOF without PTMD (Amp. (Norm.)), add the four amplitudes together, and plot them in Fig. 17. The delta, circle and square marks represent the cases of Tables 1–3, 4–6 and 7–9, respectively. The red, green and blue marks denote the cases of $X_F = 0.3\bar{l}$, $0.5\bar{l}$ and $0.7\bar{l}$, respectively. If the total of Amp. (Norm.) is less than 4, then the PTMD is considered effective; otherwise, it is considered less than ideal. Due to the large number of possible combinations, we use the IRCP (Fig. 6) as a foundation for selection and comparing the probability of internal resonance occurring within the system. In this manner, we are able to select good and poor PTMD mass ratios ($\bar{m}$) for the compilation of tables with various PTMD combinations. Take $\bar{m} = 0.1$ (green) and $\bar{m} = 0.3$ (pink) in Fig. 6 as an example. When $\bar{m} = 0.3$, the probability of internal resonance is higher (the pink portion is

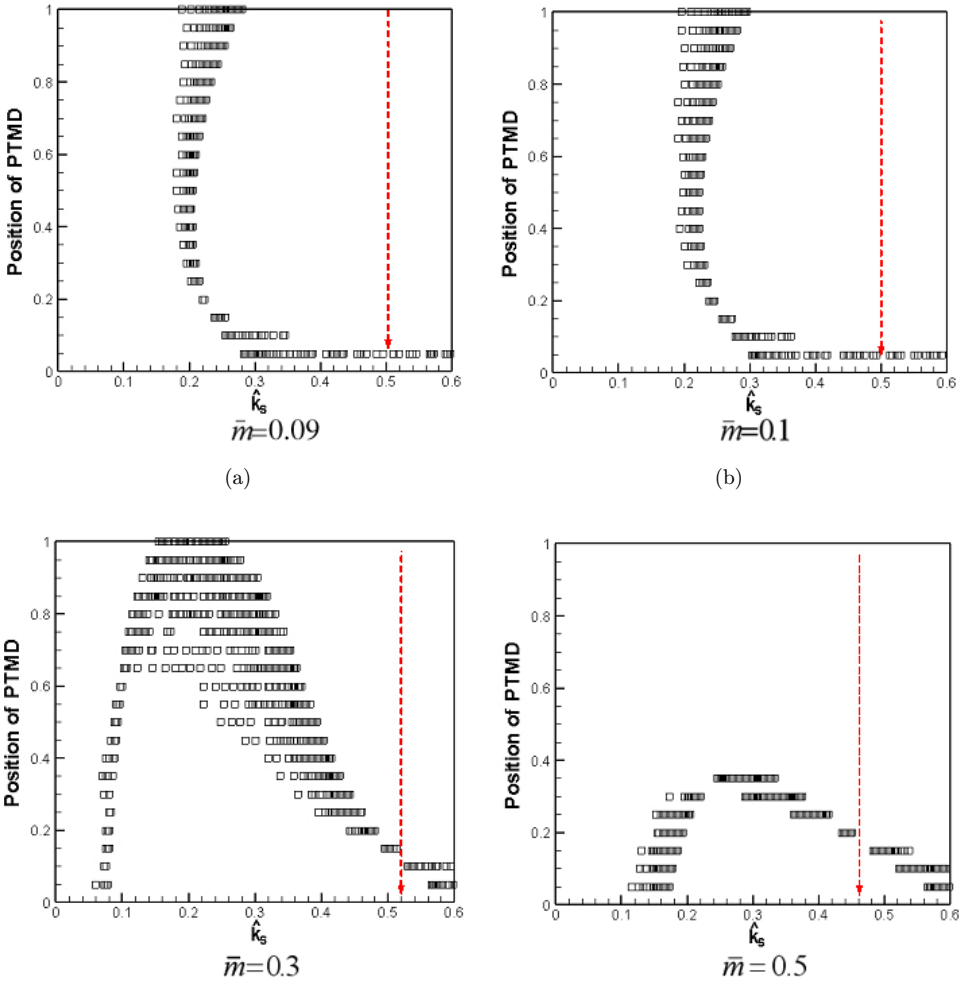

Fig. 14. 2D-IRCP on x_D–$\hat{k}_S$ plane for different $\bar{m}$. (a) $\bar{m} = 0.09$; (b) $\bar{m} = 0.1$; (c) $\bar{m} = 0.3$; (d) $\bar{m} = 0.5$.

greater than the green portion). As a result, we can identify good and poor PTMD mass ratios from Fig. 6 ($\bar{m} = 0.1$ and $\bar{m} = 0.3$) and then use the PTMD locations most capable of preventing internal resonance (see Figs. 14 and 15) for the selection of proper values for $\hat{k}_S$ and $\hat{k}_T$ and compared their damping effects.

The primary purpose of Tables 1–9 is to identify the PTMD combination with the best damping effects (including $\bar{m}$ and PTMD location). In addition, we also consider whether changing $\hat{k}_S$, $\hat{k}_T$ and the location of the PTMD can improve the effectiveness of the PTMD even with a poor mass ratio ($\bar{m}$). Tables 1–3 list the amplitudes in various DOFs in the main body with $\bar{m} = 0.1$, $\hat{k}_s = 0.5$ and $\hat{k}_T = 0.45$ when an external force is applied at $X_F = 0.3\bar{l}$, $0.5\bar{l}$ and $0.7\bar{l}$ from the mass center of the main

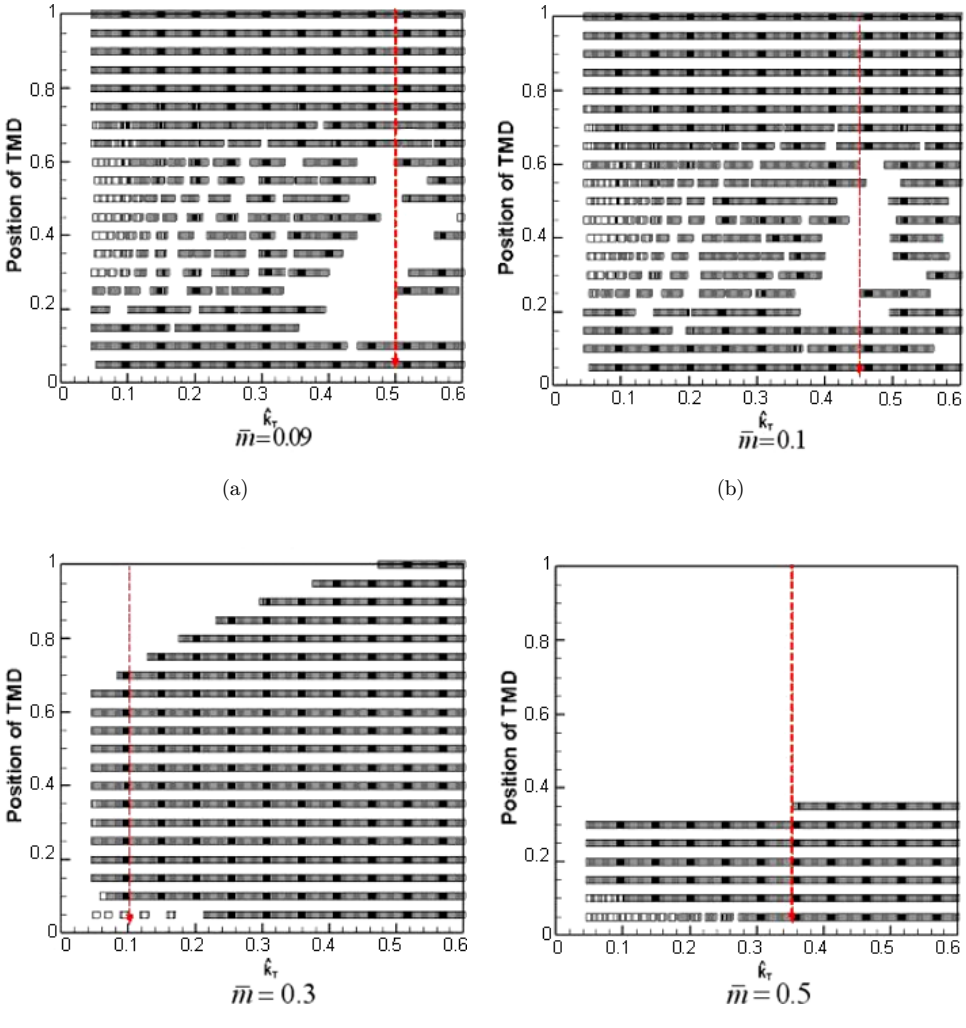

Fig. 15. 2D-IRCP on x_D–$\hat{k}_T$ plane for different $\bar{m}$. (a) $\bar{m} = 0.09$; (b) $\bar{m} = 0.1$; (c) $\bar{m} = 0.3$; (d) $\bar{m} = 0.5$.

body. Two time response plots are included on the right for verification. The combinations corresponding to these plots are marked in bold front text in the tables. With an external force applied at $X_F = 0.3\bar{l}$, $0.5\bar{l}$ and $0.7\bar{l}$ from the mass center of the main body, Tables 4–6 show the amplitudes resulting from a PTMD mass ratio deliberately selected for its high probability of internal resonance in conjunction with a combination comprising a good $\hat{k}_s = 0.52$ and a poor $\hat{k}_T = 0.5$. Tables 7–9 present the amplitudes resulting from the same conditions as those in Tables 4–6 except with a combination comprising a poor $\hat{k}_s = 0.25$ and a good $\hat{k}_T = 0.1$. In Tables 7–9, internal resonance occurred when the PTMD was more than $0.45\bar{l}$ from the left end

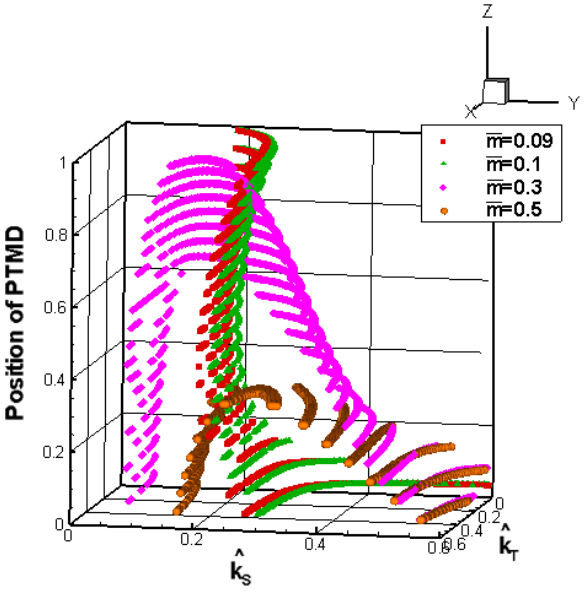

Fig. 16. 3D-IRCP for several typical $\bar{m}$.

Table 1. Amplitudes of the case of $\bar{m} = 0.1$, $\hat{k}_S = 0.5$, $\hat{k}_T = 0.45$, $X_F = 0.3$.

$\bar{m} = 0.1$, $X_F = 0.3$, $\hat{k}_s = 0.5$, $\hat{k}_T = 0.45$	Excite y-DOF		Excite θ_B-DOF		Total Amp.	Remarks
	y-Amp.	θ_B-Amp.	y-Amp.	θ_B-Amp.	Norm.	
No PTMD	2.3	1.6	1.15	0.175	4	
Posit. of TMD = 0.05	1.78	0.011	1.0×10^{-11}	0.195	1.895073758	
Posit. of TMD = 0.10	1.8	0.019	5.0×10^{-12}	0.165	1.737340839	
Posit. of TMD = 0.15	1.7	0.015	1.0×10^{-11}	0.125	1.462791149	
Posit. of TMD = 0.20	1.4	0.013	1.0×10^{-11}	0.085	1.102534938	
Posit. of TMD = 0.25	1.8	0.02	1.0×10^{-11}	0.0417	1.03339441	
Posit. of TMD = 0.30	1.85	0.021	1.0×10^{-11}	**0.003**	0.834615683	
Posit. of TMD = 0.35	1.8	0.038	1.0×10^{-11}	0.035	1.006358696	
Posit. of TMD = 0.40	1.9	0.022	1.0×10^{-11}	0.06	1.182694099	
Posit. of TMD = 0.45	1.9	0.033	1.0×10^{-11}	0.09	1.360997671	
Posit. of TMD = 0.50	1.75	0.031	1.0×10^{-11}	0.125	1.49453028	
Posit. of TMD = 0.55	1.9	0.042	1.0×10^{-11}	0.145	1.680908385	
Posit. of TMD = 0.60	1.8	0.12	1.0×10^{-11}	0.165	1.800465839	
Posit. of TMD = 0.65	1.9	0.07	1.0×10^{-11}	0.183	1.915551242	
Posit. of TMD = 0.70	1.75	0.041	1.0×10^{-11}	0.195	1.90078028	
Posit. of TMD = 0.75	2	0.16	1.0×10^{-11}	0.195	2.083850932	
Posit. of TMD = 0.80	1.95	0.17	1.0×10^{-11}	0.195	2.068361801	
Posit. of TMD = 0.85	2.1	0.175	1.0×10^{-11}	0.195	2.136704193	
Posit. of TMD = 0.90	2.3	0.17	1.0×10^{-11}	0.195	2.220535714	
Posit. of TMD = 0.95	2.2	0.162	1.0×10^{-11}	**0.195**	2.172057453	

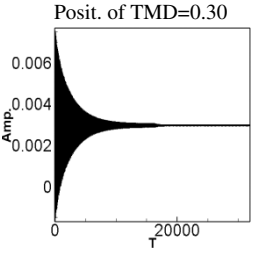

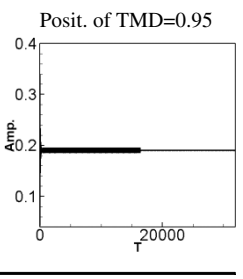

Table 2. Amplitudes of the case of $\bar{m} = 0.1$, $\hat{k}_S = 0.5$, $\hat{k}_T = 0.45$, $X_F = 0.5$.

$\bar{m} = 0.1$, $X_F = 0.5$, $\hat{k}_s = 0.5$, $\hat{k}_T = 0.45$	Excite y-DOF		Excite θ_B-DOF		Total Amp. Norm.	Remarks
	y-Amp.	θ_B-Amp.	y-Amp.	θ_B-Amp.		
No PTMD	2.3	1.6	1.68	0.265	4	
Posit. of TMD = 0.05	1.78	0.011	1.0×10^{-7}	0.28	1.838541568	
Posit. of TMD = 0.10	1.8	0.019	1.0×10^{-7}	0.25	1.736498809	
Posit. of TMD = 0.15	1.7	0.015	1.0×10^{-7}	0.19	1.465062244	
Posit. of TMD = 0.20	1.41	0.013	1.3×10^{-7}	0.14	1.148567665	
Posit. of TMD = 0.25	1.8	0.02	1.0×10^{-7}	0.069	1.051319447	
Posit. of TMD = 0.30	1.65	0.021	1.0×10^{-7}	**0.005**	0.745456819	
Posit. of TMD = 0.35	1.8	0.038	1.0×10^{-7}	0.058	1.010612482	
Posit. of TMD = 0.40	1.9	0.022	1.0×10^{-7}	0.11	1.246736911	
Posit. of TMD = 0.45	1.9	0.033	1.0×10^{-7}	0.16	1.439613687	
Posit. of TMD = 0.50	1.75	0.031	1.0×10^{-7}	0.205	1.54371379	
Posit. of TMD = 0.55	1.9	0.042	1.0×10^{-7}	0.24	1.741191838	
Posit. of TMD = 0.60	1.8	0.12	1.0×10^{-7}	0.26	1.772321078	
Posit. of TMD = 0.65	1.9	0.07	1.0×10^{-7}	0.31	2.001762534	
Posit. of TMD = 0.70	2.1	0.041	1.0×10^{-7}	0.33	2.168511742	
Posit. of TMD = 0.75	1.95	0.16	1.0×10^{-7}	0.36	2.215575972	
Posit. of TMD = 0.80	1.95	0.17	1.0×10^{-7}	0.382	2.299520766	
Posit. of TMD = 0.85	2.1	0.175	1.0×10^{-7}	0.4	2.431119475	
Posit. of TMD = 0.90	2.3	0.17	1.0×10^{-7}	0.41	2.557355056	
Posit. of TMD = 0.95	2.2	0.162	1.0×10^{-7}	**0.42**	2.550810175	

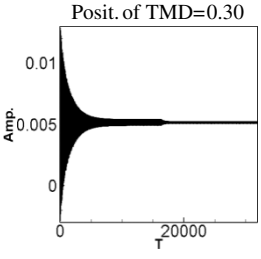

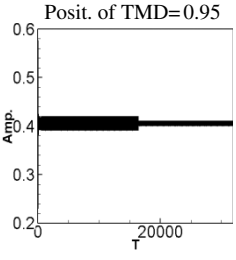

of the main body. To better observe the influence of internal resonance on the amplitude of the system, we excite the first DOF (y-DOF), which results in greater amplitudes in the first DOF than in the second DOF. When we excite the second DOF (θ_B-DOF), the amplitudes in the first DOF are still greater than those in the second DOF. The peak amplitudes in the system with the PTMD at various locations are recorded in Table 7. To save space, we list only the amplitude data from Tables 8 and 9, in which internal resonance is prevented.

From Tables 1–9, one observes that when the excitation is at y-DOF (in the transverse direction) with various combinations of the PTMD and locations of applied force, the PTMD location nearest the mass center ($0.17837\bar{l}$) exerts the greatest damping effects for the y-DOF. In other words, the PTMD located at $0.2\bar{l}$ contributes to the smallest transverse amplitude in the main body in Tables 1–9. Using a PTMD mass ratio of $\bar{m} = 0.1$ and excitation of the θ_B-DOF, the PTMD located at $0.3\bar{l}$ from the left end of the main body exerts the most pronounced damping effects, regardless of where the external force is applied. If the PTMD is moved away from this location in either direction, the damping effects are diminished. This is likely due to the fact the PTMD is below the mass center, whereby the PTMD mass ratio ($\bar{m}$) and the form of rotation cannot be used for damping. Clearly, the PTMD must be slightly away from the mass center for it to have an effective lever arm with which to balance vibrations. Nevertheless, if the lever arm is too long, then the vibration reduction effects are diminished. Overall, the combinations with $\bar{m} = 0.1$ have the best

Table 3. Amplitudes of the case of $\bar{m} = 0.1$, $\hat{k}_S = 0.5$, $\hat{k}_T = 0.45$, $X_F = 0.7$.

$\bar{m} = 0.1$, $X_F = 0.7$, $\hat{k}_s = 0.5$, $\hat{k}_T = 0.45$	Excite y-DOF		Excite θ_B-DOF		Total Amp.	Remarks
	y-Amp.	θ_B-Amp.	y-Amp.	θ_B-Amp.	Norm.	
No PTMD	2.3	1.63	2.1	0.41	4	Posit. of TMD=0.30
Posit. of TMD = 0.05	1.77	0.013	1.0×10^{-11}	0.57	2.16778458	
Posit. of TMD = 0.10	1.8	0.016	1.9×10^{-11}	0.39	1.743644159	
Posit. of TMD = 0.15	1.7	0.015	6.7×10^{-11}	0.26	1.38247923	
Posit. of TMD = 0.20	1.41	0.018	1.0×10^{-11}	0.2	1.111891301	
Posit. of TMD = 0.25	1.8	0.02	1.0×10^{-11}	0.1	1.038781073	
Posit. of TMD = 0.30	1.85	0.02	1.0×10^{-11}	**0.0079**	0.835886057	
Posit. of TMD = 0.35	1.8	0.038	1.0×10^{-11}	0.08	1.00104353	
Posit. of TMD = 0.40	1.9	0.0225	1.0×10^{-11}	0.15	1.205744296	
Posit. of TMD = 0.45	1.9	0.0325	1.3×10^{-11}	0.23	1.407001217	
Posit. of TMD = 0.50	1.75	0.031	6.0×10^{-11}	0.298	1.506717238	
Posit. of TMD = 0.55	1.9	0.041	1.0×10^{-11}	0.32	1.631728136	Posit. of TMD=0.95
Posit. of TMD = 0.60	1.8	0.0425	1.0×10^{-11}	0.41	1.808682315	
Posit. of TMD = 0.65	1.6	0.041	1.0×10^{-11}	0.441	1.796415304	
Posit. of TMD = 0.70	1.75	0.04	1.0×10^{-11}	0.5	2.004921638	
Posit. of TMD = 0.75	2	0.08	1.0×10^{-11}	0.54	2.235718143	
Posit. of TMD = 0.80	1.95	0.0525	1.0×10^{-11}	0.55	2.221498091	
Posit. of TMD = 0.85	2.1	0.13	1.0×10^{-11}	0.56	2.358651738	
Posit. of TMD = 0.90	2.3	0.061	1.0×10^{-11}	0.58	2.452057459	
Posit. of TMD = 0.95	2.2	0.165	1.0×10^{-11}	**0.605**	2.533358489	

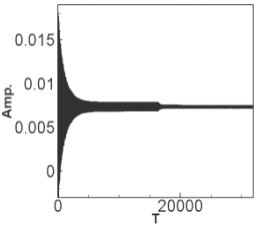

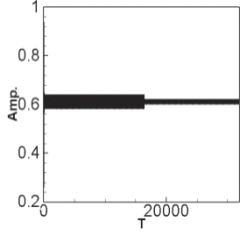

damping effects. Adjusting the location of the PTMD can result in a Total Amp. (Norm.) of 0.75, which indicates that the amplitudes of the main body can be reduced to $(0.75/4) \approx 18.75\%$.

Although the IRCP provides combinations capable of preventing internal resonance, it cannot guarantee good damping effects when internal resonance does not occur. Tables 1–9 illustrate that a PTMD mass ratio of $\bar{m} = 0.3$ is not a good combination to reduce vibrations. This is because larger $\bar{m}$ values mean that the addition of the PTMD to the main body can change the system's mass center. Although this somehow prevents internal resonance, larger $\bar{m}$ values are also less economical; sensitivity to rotation is heightened, and the overall damping effect is reduced. Tables 4–9 show the damping effects of various combinations with $\bar{m} = 0.3$. From the IRCP, we can see that $\bar{m} = 0.3$ is not necessarily a good choice for cases involving internal resonance. The tables also indicate that these combinations are ineffective in vibration reduction.

If the external force excites the θ_B-DOF, PTMD locations further away from the left end of the main body, better damping effect can be achieved, regardless of where the force is applied (excluding the combinations in which internal resonance occurs). When $\bar{m} = 0.3$, the Total Amp. (Norm.) can be reduced as low as 3.66 (Table 6, position of $PTMD = 0.95$). In other words, it can reduce the amplitudes by $(4 - 3.66)/4 = 8.5\%$, and under adverse conditions, the overall amplitudes can be decreased through selection of appropriate parameters. Even though the damping

Table 4. Amplitudes of the case of $\bar{m} = 0.3$, $\hat{k}_S = 0.52$, $\hat{k}_T = 0.5$, $X_F = 0.3$.

$\bar{m} = 0.3$, $X_F = 0.3$, $\hat{k}_s = 0.52$, $\hat{k}_T = 0.5$	Excite y-DOF		Excite θ_B-DOF		
	y-Amp.	θ_B-Amp.	y-Amp.	θ_B-Amp.	Total Amp. Norm.
No PTMD	2.3	1.6	1.15	0.175	4
Posit. of TMD = 0.05	2.8	0.25	0	0.96	6.85935559
Posit. of TMD = 0.10	3.1	0.21	0.1	0.84	6.366032609
Posit. of TMD = 0.15	2.75	0.2	0	0.82	6.00636646
Posit. of TMD = 0.20	2.7	0.13	0.102	0.8	5.915287267
Posit. of TMD = 0.25	2.8	0.17	0	0.8	5.895069876
Posit. of TMD = 0.30	3.1	0	0.101	0.8	6.007080745
Posit. of TMD = 0.35	3.1	0.08	0	0.76	5.74068323
Posit. of TMD = 0.40	2.75	0.1	0.1	0.76	5.687965839
Posit. of TMD = 0.45	2.87	0.1	0	0.74	5.538897516
Posit. of TMD = 0.50	2.95	0.07	0.096	0.74	5.638408385
Posit. of TMD = 0.55	2.87	0.1	0	0.72	5.424611801
Posit. of TMD = 0.60	2.95	0.05	0.1	0.69	5.34367236
Posit. of TMD = 0.65	3.1	0.05	0.095	0.69	5.404541925
Posit. of TMD = 0.70	3.05	0.05	0.047	0.66	5.169635093
Posit. of TMD = 0.75	3.28	0.06	0.1	0.62	5.093400621
Posit. of TMD = 0.80	2.9	0.19	0	0.58	4.69390528
Posit. of TMD = 0.85	3.3	0.13	0	0.56	4.716032609
Posit. of TMD = 0.90	3	0.12	0	0.53	4.407919255
Posit. of TMD = 0.95	3.05	0.15	0	0.51	4.334122671

Table 5. Amplitudes of the case of $\bar{m} = 0.3$, $\hat{k}_S = 0.524$, $\hat{k}_T = 0.5$, $X_F = 0.5$.

$\bar{m} = 0.3$, $X_F = 0.5$, $\hat{k}_s = 0.52$, $\hat{k}_T = 0.5$	Excite y-DOF		Excite θ_B-DOF		
	y-Amp.	θ_B-Amp.	y-Amp.	θ_B-Amp.	Total Amp. Norm.
No PTMD	2.3	1.62	1.68	0.265	4
Posit. of TMD = 0.05	2.8	0.25	1.0×10^{-5}	1.2	5.900020131
Posit. of TMD = 0.10	3.1	0.21	1.0×10^{-5}	1.15	5.81708431
Posit. of TMD = 0.15	2.75	0.2	1.0×10^{-5}	1.1	5.470058313
Posit. of TMD = 0.20	2.7	0.13	1.3×10^{-5}	1.1	5.405109306
Posit. of TMD = 0.25	2.8	0.17	1.0×10^{-5}	1.08	5.397807226
Posit. of TMD = 0.30	3.2	0	1.0×10^{-5}	0.992	5.134706527
Posit. of TMD = 0.35	3.1	0.08	1.0×10^{-5}	0.99	5.133063812
Posit. of TMD = 0.40	2.75	0.1	1.0×10^{-5}	0.99	4.993235578
Posit. of TMD = 0.45	2.87	0.1	1.0×10^{-5}	0.97	4.969937793
Posit. of TMD = 0.50	2.95	0.07	1.0×10^{-5}	0.96	4.948466034
Posit. of TMD = 0.55	2.87	0.1	1.0×10^{-5}	0.96	4.932201944
Posit. of TMD = 0.60	2.95	0.05	8.5×10^{-5}	0.9	4.709749904
Posit. of TMD = 0.65	3.1	0.05	3.1×10^{-5}	0.88	4.699463454
Posit. of TMD = 0.70	3.05	0.05	1.0×10^{-5}	0.88	4.677711823
Posit. of TMD = 0.75	3.28	0.06	1.0×10^{-5}	0.85	4.670677116
Posit. of TMD = 0.80	2.9	0.19	1.0×10^{-5}	0.81	4.434763242
Posit. of TMD = 0.85	3.3	0.13	1.0×10^{-5}	0.77	4.420695852
Posit. of TMD = 0.90	3	0.12	1.0×10^{-5}	0.77	4.28408823
Posit. of TMD = 0.95	3.05	0.15	1.0×10^{-5}	0.75	4.248874181

Table 6. Amplitudes of the case of $\bar{m} = 0.3$, $\hat{k}_S = 0.52$, $\hat{k}_T = 0.5$, $X_F = 0.7$.

$\bar{m} = 0.3$, $X_F = 0.7$, $\hat{k}_s = 0.52$, $\hat{k}_T = 0.5$	Excite y-DOF		Excite θ_B-DOF		
	y-Amp.	θ_B-Amp.	y-Amp.	θ_B-Amp.	Total Amp. Norm.
No PTMD	2.3	1.63	2.1	0.41	4
Posit. of TMD = 0.05	2.85	0.25	0	1.35	4.685187595
Posit. of TMD = 0.10	3	0.21	0.17	1.3	4.68486627
Posit. of TMD = 0.15	2.8	0.2	0.12	1.25	4.446014036
Posit. of TMD = 0.20	2.7	0.13	0.1	1.25	4.35006718
Posit. of TMD = 0.25	2.85	0.17	0	1.218	4.34950573
Posit. of TMD = 0.30	3.1	0	0	1.21	4.346664647
Posit. of TMD = 0.35	2.98	0.08	0.1	1.21	4.343570488
Posit. of TMD = 0.40	2.87	0.1	0	1.21	4.30801434
Posit. of TMD = 0.45	2.87	0.1	0.1	1.21	4.30801434
Posit. of TMD = 0.50	2.95	0.07	0	1.21	4.276772993
Posit. of TMD = 0.55	2.87	0.1	0.1	1.13	4.112892389
Posit. of TMD = 0.60	2.98	0.05	0	1.08	3.960473362
Posit. of TMD = 0.65	3	0.05	0.11	1.05	3.948379235
Posit. of TMD = 0.70	3.05	0.05	0.14	1.03	3.926099782
Posit. of TMD = 0.75	3.2	0.06	0.11	1	3.919519506
Posit. of TMD = 0.80	2.9	0.19	0.11	0.97	3.798736078
Posit. of TMD = 0.85	3.1	0.13	0.11	0.95	3.797034811
Posit. of TMD = 0.90	3	0.12	0.11	0.92	3.674250849
Posit. of TMD = 0.95	3.05	0.15	0.1	0.9	3.660852495

Table 7. Amplitudes of the case of $\bar{m} = 0.3$, $\hat{k}_S = 0.25$, $\hat{k}_T = 0.1$, $X_F = 0.3$.

$\bar{m} = 0.3$, $X_F = 0.3$, $\hat{k}_s = 0.25$, $\hat{k}_T = 0.1$	Excite y-DOF		Excite θ_B-DOF		
	y-Amp.	θ_B-Amp.	y-Amp.	θ_B-Amp.	Total Amp. Norm.
No PTMD	2.3	1.6	1.15	0.175	4
Posit. of TMD = 0.05	4.05	0.13	0.11	0.88	6.966343168
Posit. of TMD = 0.10	3.6	0.32	0.1	0.86	6.766459627
Posit. of TMD = 0.15	3.5	0.3	0.13	0.84	6.622282609
Posit. of TMD = 0.20	3.4	0.28	0.1	0.82	6.434627329
Posit. of TMD = 0.25	3.7	0.26	0.1	0.81	6.430745342
Posit. of TMD = 0.30	3.4	0.24	0.1	0.8	6.286645963
Posit. of TMD = 0.35	3.7	0.2	0.1	0.77	6.220652174
Posit. of TMD = 0.40	3.7	0.2	0.1	0.77	6.220652174
Posit. of TMD = 0.45	3.7	0.17	0.1	0.75	6.08761646
Posit. of TMD = 0.50	3.8	0.16	1.75	0.75	7.559627329
Posit. of TMD = 0.55	3.7	0.16	1.9	0.65	7.07515528
Posit. of TMD = 0.60	4	0	1.76	0.63	6.869565217
Posit. of TMD = 0.65	3.8	0.11	1.85	0.6	6.758190994
Posit. of TMD = 0.70	3.81	0.14	1.07	0.59	6.045885093
Posit. of TMD = 0.75	3.81	0.1	2	0.58	6.772437888
Posit. of TMD = 0.80	3.81	0	2	0.58	6.709937888
Posit. of TMD = 0.85	3.8	0.17	1.9	0.53	6.439169255
Posit. of TMD = 0.90	4	0	1.7	0.53	6.245962733
Posit. of TMD = 0.95	4.2	0.16	1.95	0.5	6.478881988

Table 8. Amplitudes of the case of $\bar{m} = 0.3$, $\hat{k}_S = 0.25$, $\hat{k}_T = 0.1$, $X_F = 0.5$.

$\bar{m} = 0.3$, $X_F = 0.5$, $\hat{k}_s = 0.25$, $\hat{k}_T = 0.1$	Excite y-DOF		Excite θ_B-DOF		
	y-Amp.	θ_B-Amp.	y-Amp.	θ_B-Amp.	Total Amp. Norm.
No PTMD	2.3	1.62	1.68	0.265	4
Posit. of TMD = 0.05	4.05	0.13	0.1	1.12	6.127055383
Posit. of TMD = 0.10	3.6	0.32	0.135	1.1	5.994048795
Posit. of TMD = 0.15	3.5	0.3	0.1	1.08	5.841919823
Posit. of TMD = 0.20	3.4	0.28	0.105	1.08	5.789072074
Posit. of TMD = 0.25	3.7	0.26	0.1	1.05	5.79097744
Posit. of TMD = 0.30	3.4	0.24	0.11	1.02	5.540941812
Posit. of TMD = 0.35	3.6	0.2	0.1	1	5.521782897
Posit. of TMD = 0.40	3.81	0.2	0.1	0.97	5.499879697
Posit. of TMD = 0.45	3.7	0.17	0.1	0.95	5.358063394

effect is less than ideal, internal resonance can still be prevented. We can see that altering the position of the PTMD still plays an important role in vibration reduction.

4.2.3. *Effect of PTMD mass ratio ($\bar{m}$) and other parameters*

The effect of variance in $\bar{m}$ on the damping effect in the system is also worth discussing (Fig. 18). Figure 18 shows the normalized total amplitudes resulting from the case when $\bar{m} = 0.5$ (square marks) and the force is applied at $X_F = 0.3\bar{l}$ (red marks), $0.5\bar{l}$ (green marks), and $0.7\bar{l}$ (blue marks) from the mass center of the main body. Based on Figs. 14 and 15, we select the combination of $\hat{k}_s = 0.46$ and $\hat{k}_T = 0.35$. The first objective is to use the IRCP to prevent internal resonance and list the various amplitudes using the frequency responses before comparing their damping effects. Figure 18 also shows the resulting amplitudes when $\bar{m} = 0.09$ (circle marks) and the force is applied at $X_F = 0.3\bar{l}$ (red marks), $0.5\bar{l}$ (green marks) and $0.7\bar{l}$

Table 9. Amplitudes of the case of $\bar{m} = 0.3$, $\hat{k}_S = 0.25$, $\hat{k}_T = 0.1$, $X_F = 0.7$.

$\bar{m} = 0.3$, $X_F = 0.7$, $\hat{k}_s = 0.25$, $\hat{k}_T = 0.1$	Excite y-DOF		Excite θ_B-DOF		
	y-Amp.	θ_B-Amp.	y-Amp.	θ_B-Amp.	Total Amp. Norm.
No PTMD	2.3	1.63	2.1	0.41	4
Posit. of TMD = 0.05	4.05	0.13	0	1.35	5.133307093
Posit. of TMD = 0.10	3.6	0.32	0.135	1.33	5.069724563
Posit. of TMD = 0.15	3.5	0.3	0.1	1.27	4.850968233
Posit. of TMD = 0.20	3.3	0.28	0.11	1.25	4.70772319
Posit. of TMD = 0.25	3.5	0.26	0.1	1.21	4.680086893
Posit. of TMD = 0.30	3.4	0.24	0.145	1.2	4.621377021
Posit. of TMD = 0.35	3.6	0.2	0.12	1.17	4.598718172
Posit. of TMD = 0.40	3.81	0.2	0.115	1.13	4.590080591
Posit. of TMD = 0.45	3.7	0.17	0.13	1.13	4.530992454

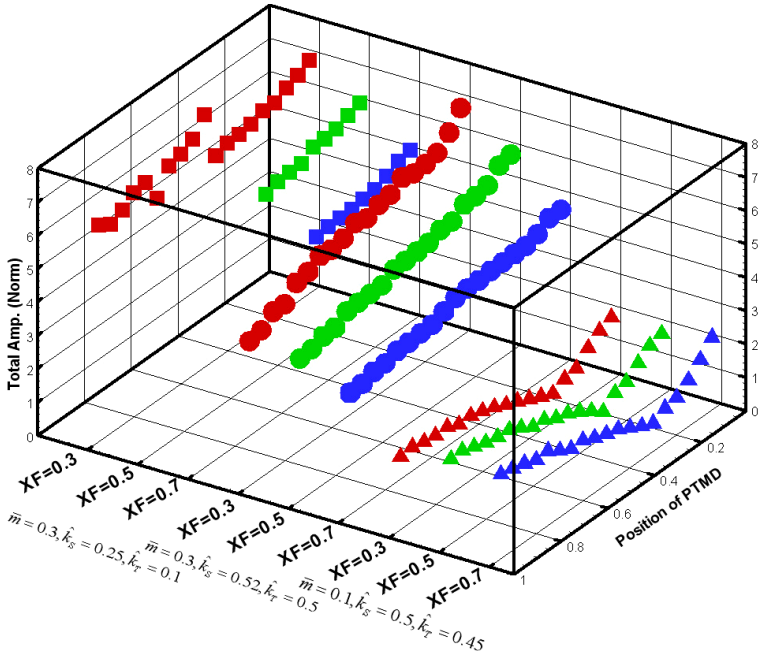

Fig. 17. Normalized total Amp. for $\bar{m} = 0.1$ and 0.3.

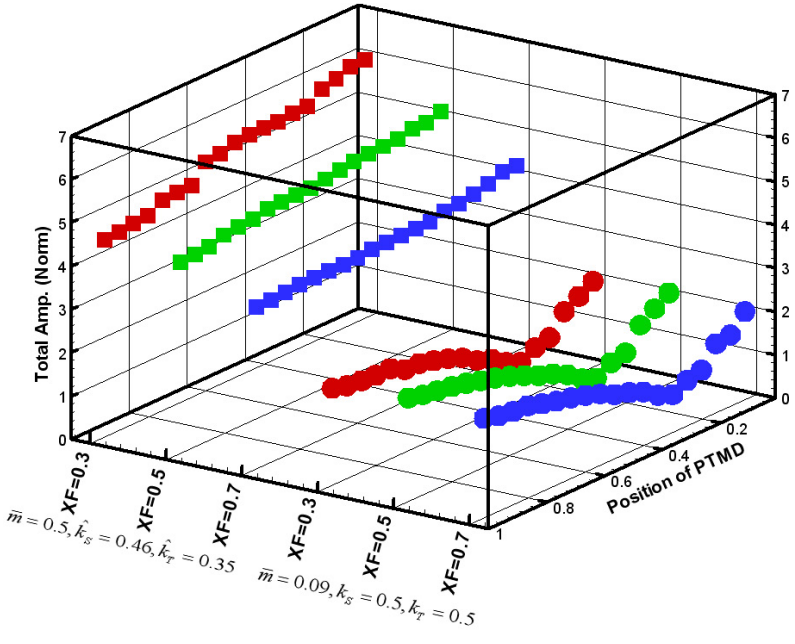

Fig. 18. Normalized total Amp. for $\bar{m} = 0.5$ and 0.09.

(blue marks) from the mass center of the main body. Based on Figs. 14 and 15, we select the combination of $\hat{k}_s = 0.5$ and $\hat{k}_T = 0.5$. Among the various PTMD mass ratios, we discover that both $\bar{m}$ values are too large and those that are too small have an adverse effect on damping. If the $\bar{m}$ is too large, then the system frequency can be altered, which can effectively prevent internal frequency. However, this does not benefit vibration reduction. Generally speaking, the entire system is dominated by the main body, however, if $\bar{m}$ is too large, then the PTMD may dominate the system instead. From an economic perspective, this is not a very good design concept. In contrast, if the $\bar{m}$ is too small, such as 0.09, the damping effects is not necessarily better than the case with $\bar{m} = 0.1$, but they are better than the cases with $\bar{m} = 0.3$ or 0.5. This implies that too small or too large $\bar{m}$ values do not reveal better damping effect. Through observation, we discover that $\bar{m} = 0.1$ is the best PTMD mass ratio, capable of preventing internal resonance and providing excellent damping effects. It is evident that the proposed method of creating an IRCP and sequentially selecting PTMD parameters provides considerable reference value.

In Sec. 4.2.1, we observed that changing $\hat{k}_T$ is ineffective in preventing internal resonance. Its influence on vibration in the main body is outlined in Table 10. Take $\bar{m} = 0.1$ as an example: By adopting fixed values for $\hat{k}_S$ or $\hat{k}_T$, we can observe the influence of changing $\hat{k}_T$ or $\hat{k}_S$ on the amplitude. The upper half of Table 10 shows the influence of changing $\hat{k}_T$ on the damping effect. On the one hand, as $\hat{k}_T$ increases from 0.1 to 0.45, the damping effect is not significant even though the transverse amplitudes from excitation to the the y-DOF decrease. On the other hand, the θ_B amplitudes resulting from excitation to the θ_B-DOF decrease (from 0.021 to 0.003). The lower half of Table 10 shows the influence of changing $\hat{k}_S$ on the damping effect. As $\hat{k}_S$ increases from 0.2 to 0.5, the transverse amplitudes resulting from excitation to the y-DOF decrease. However, the damping effect is insignificant. In contrast, the θ_B amplitudes from excitation to the θ_B-DOF drops significantly (from 1.2 to 0.003). From this, we discover that in terms of the θ_B-DOF, changing $\hat{k}_S$ is much more

Table 10. Amplitudes of the case of $\bar{m} = 0.1$, $X_F = 0.3$, for different spring constants.

	Excite y-DOF		Excite θ_B-DOF		
	y-Amp.	θ_B-Amp.	y-Amp.	θ_B-Amp.	Total Amp. Norm.
$\bar{m} = 0.1$, $X_F = 0.3$, $\hat{k}_s = 0.5$, Posit. of TMD $= 0.3$					
No $\hat{k}_T$	2.1	0.022	2.0×10^{-10}	0.051	2.17
$\hat{k}_T = 0.1$	1.92	0.013	5.0×10^{-7}	0.021	1.95
$\hat{k}_T = 0.25$	1.9	0.01	3.0×10^{-11}	0.009	1.92
$\hat{k}_T = 0.45$	1.85	0.021	1.0×10^{-11}	0.003	1.87
$\bar{m} = 0.1$, $X_F = 0.3$, $\hat{k}_T = 0.45$, Posit. of TMD $= 0.3$					
$\hat{k}_s = 0.2$	1.9	0.02	3.0×10^{-11}	1.2	3.12
$\hat{k}_s = 0.35$	1.87	0.022	1.0×10^{-11}	0.0072	1.9
$\hat{k}_s = 0.5$	1.85	0.021	1.0×10^{-11}	0.003	1.87

effective than changing $\hat{k}_T$ with regard to vibration reduction. However, in the transverse direction, the influence is not as pronounced.

Furthermore, unlike general PTMDs in which only a single extension spring connects the PTMD to the main body, this study proposes the use of a torsion spring and extension spring to connect the two. Added to the fact that the torsion spring transforms the damping system into a 2D PTMD, the frequency of the overall system is altered (which prevents internal resonance), thereby inhibiting vibrations in the transverse and rotational directions. Take $\bar{m} = 0.1$ as an example (Table 10), the addition of the torsion spring resulting in total amplitudes of $(1.87/2.17) \approx 86.18\%$ of those without the torsion spring. This demonstrates the effectiveness of adding a torsion spring as a design device.

5. Conclusion

This study investigated a slender rigid body in vibration with 1:2 internal resonance, exploring the influence of various damper parameters on damping effects and the occurrence of internal resonance in the system. The instruments used include Fixed Points Plots, time response and Poincaré maps, which were compared for confirmation of accuracy. Moreover, we proposed a 3D-IRCP aided by various amplitude analysis tables for the identification of PTMD parameter combinations capable of preventing internal resonance. This approach also enables designers to evaluate the effectiveness of various parameter combinations of the PTMD prior to the design process, in that the most effective PTMD parameters can be obtained in an economical manner by only altering the location of the PTMD. The findings of this study are summarized as follows:

(1) This study indicated that $\bar{m} = 0.1$ is the best PTMD mass ratio. In addition to preventing internal resonance, vibration amplitudes in the main body can also be reduced to 18.75% under certain PTMD parameter combinations.
(2) With the same PTMD mass ratio, merely changing the extension spring constant and torsion spring constant can also prevent internal resonance.
(3) With a fixed PTMD mass ratio, extension spring constant, and torsion spring constant, we can also alter the location of the PTMD to prevent internal resonance and reduce vibration.
(4) The use of a torsion spring as well as an extension spring for connections resulted in a total amplitude of only 86.18% of that without a torsion spring, demonstrating the effectiveness of this approach as a design aid.
(5) This study also proposed a procedure for the selection of PTMD parameters, which involves selecting damper parameters using the 3D-IRCP to prevent internal resonance for the creation of amplitude analysis tables for vibration reduction. This procedure is an economical approach meant to enable designers to evaluate the effectiveness of PTMDs quickly and precisely.

Appendix A

$$\bar{m}=\frac{m}{M},\quad \bar{y}=\frac{y}{l},\quad \bar{u}=\frac{u}{l},\quad \bar{l}_1=\frac{l_1}{l},\quad \bar{l}_2=\frac{l_2}{l},\quad \bar{l}_A=\frac{l_A}{l},\quad \bar{x}_A=\frac{x_A}{l},$$

$$\varepsilon\bar{\alpha}=\alpha l^2,\quad \varepsilon\bar{\beta}=\beta l^2,\quad \varepsilon\xi_y=\frac{2C}{\sqrt{2KM}},\quad \varepsilon\bar{\Delta}=\Delta,\quad \varepsilon\xi_{\theta_B}=\frac{Cl^2}{I_B\omega_y},\quad \hat{k}_s=\frac{k_s}{2K},$$

$$\hat{k}_T=\frac{k_T}{2Kl^2},\quad \omega_y=\sqrt{\frac{2K}{M}},\quad \omega_{\theta_B}=\sqrt{\frac{Kl^2}{I_B}},\quad \omega_u=\sqrt{\frac{k_s}{m}},\quad \omega_{\theta_A}=\sqrt{\frac{k_T}{I_A}},$$

$$\omega_{PD}=\sqrt{\frac{g}{l_A}},\quad \bar{\omega}_{\theta_B}=\frac{\omega_{\theta_B}}{\omega_y},\quad \bar{\omega}_u=\frac{\omega_u}{\omega_y},\quad \bar{\omega}_{\theta_A}=\frac{\omega_{\theta_A}}{\omega_y},\quad \bar{\omega}_{PD}=\frac{\omega_{PD}}{\omega_y},$$

$$\frac{\partial y}{\partial t}=\dot{y},\quad \frac{\partial\theta_B}{\partial t}=\dot{\theta}_B,\quad \frac{\partial u}{\partial t}=\dot{u},\quad \frac{\partial\theta_A}{\partial t}=\dot{\theta}_A,\quad T_0=\tau=\omega t,\quad \partial t=\frac{\partial\tau}{\omega},$$

$$I_A=\frac{ml_A^2}{3},\quad I_B=\frac{Ml^2}{12}+M\left(\frac{l}{2}-l_1\right)^2,\quad \bar{f}_y=f/2Kl,\quad \bar{M}_{\theta_B}=M_{\theta_B}/I_B\omega_y^2.$$

Appendix B

$$P_1=1,\quad P_5=\xi_y,\quad P_6=\left(\frac{\xi_y\bar{l}_1}{4}-\frac{\xi_y\bar{l}_2}{4}\right),\quad P_9=(1+\hat{k}_s),$$

$$P_{10}=\left(\frac{\bar{l}_1-\bar{l}_2}{2}+\hat{k}_s\bar{x}_A\right),\quad P_{11}=-\hat{k}_s,\quad P_{13}=-24\hat{k}_s\bar{\alpha}\bar{x}_A,\quad P_{14}=0,$$

$$P_{15}=-12\bar{\alpha}\hat{k}_s\bar{x}_A^2,\quad P_{16}=(6(\bar{\beta}\bar{l}_1-\bar{\beta}\bar{l}_2)+12\hat{k}_s\bar{\alpha}\bar{x}_A),\quad P_{17}=12\hat{k}_s\bar{\alpha}\bar{x}_A,$$

$$P_{18}=-12\hat{k}_s\bar{\alpha},\quad P_{19}=-12\hat{k}_s\bar{\alpha}\bar{x}_A^2,\quad P_{20}=12\hat{k}_s\bar{\alpha},\quad P_{21}=(4\bar{\beta}+4\hat{k}_s\bar{\alpha}),$$

$$P_{24}=\left((2\bar{\beta}\bar{l}_1^3-2\bar{\beta}\bar{l}_2^3)-\frac{\bar{l}_1-\bar{l}_2}{12}-\frac{1}{6}\hat{k}_s\bar{x}_A+4\hat{k}_s\bar{\alpha}\bar{x}_A^3\right),\quad P_{26}=-4\hat{k}_s\bar{\alpha},$$

$$P_{27}=(6(\bar{\beta}\bar{l}_1{}^2+\bar{\beta}\bar{l}_2{}^2)+12\hat{k}_s\bar{\alpha}\bar{x}_A^2),\quad P_2=P_3=P_4=P_7=P_8=P_{12}=0,$$

$$Q_2=1,\quad Q_5=(\xi_{\theta_B}\bar{l}_1-\xi_{\theta_B}\bar{l}_2),\quad Q_6=(\xi_{\theta_B}\bar{l}_1^2+\xi_{\theta_B}\bar{l}_2^2),$$

$$Q_9=(\bar{\omega}_{\theta_B}^2\bar{l}_1-\bar{\omega}_{\theta_B}^2\bar{l}_2+6\hat{k}_s\bar{x}_A),\quad Q_{10}=(\bar{\omega}_{\theta_B}^2(\bar{l}_1^2+\bar{l}_2^2)+12\hat{k}_T+6\hat{k}_s\bar{x}_A^2),$$

$$Q_{11}=-6\hat{k}_s\bar{x}_A,\quad Q_{12}=-12\hat{k}_T,\quad Q_{13}=-48\bar{\omega}_{\theta_B}^2\hat{k}_s\bar{\beta}\bar{x}_A^2,$$

$$Q_{16}=12\bar{\omega}_{\theta_B}^2\bar{\beta}(\bar{l}_1^2+\bar{l}_2^2)+24\bar{\omega}_{\theta_B}^2\hat{k}_s\bar{\beta}\bar{x}_A^2,\quad Q_{17}=24\bar{\omega}_{\theta_B}^2\hat{k}_s\bar{\beta}\bar{x}_A^2,$$

$$Q_{18}=-24\bar{\omega}_{\theta_B}^2\hat{k}_s\bar{\beta}\bar{x}_A,\quad Q_{19}=3\hat{k}_s\bar{x}_A-24\bar{\omega}_{\theta_B}^2\hat{k}_s\bar{\beta}\bar{x}_A^3,\quad Q_{20}=24\bar{\omega}_{\theta_B}^2\hat{k}_s\bar{\beta}\bar{x}_A,$$

$$Q_{21}=4\bar{\omega}_{\theta_B}^2\bar{\beta}(\bar{l}_1+\bar{l}_2)+8\bar{\omega}_{\theta_B}^2\hat{k}_s\bar{\beta}\bar{x}_A,$$

$$Q_{24}=-\frac{2}{3}\bar{\omega}_{\theta_B}^2(\bar{l}_1^2+\bar{l}_2^2)+4\bar{\omega}_{\theta_B}^2\bar{\beta}(\bar{l}_1^4+\bar{l}_2^4)+48\hat{k}_T\bar{\Delta}-4\hat{k}_s\bar{x}_A^2,\quad Q_{26}=-8\bar{\omega}_{\theta_B}^2\hat{k}_s\bar{\beta}\bar{x}_A,$$

$$Q_{27} = \bar{\omega}^2_{\theta_B} \frac{-\bar{l}_1 + \bar{l}_2}{2} - 3\hat{k}_s \bar{x}_A + 12\bar{\omega}^2_{\theta_B} \bar{\beta}(\bar{l}_1^3 + \bar{l}_2^3) + 24\bar{\omega}^2_{\theta_B} \hat{k}_s \bar{\beta} \bar{x}_A^3,$$

$$Q_{28} = 48\hat{k}_T \bar{\Delta}, \quad Q_{29} = -48\hat{k}_T \bar{\Delta}, \quad Q_{30} = -48\hat{k}_T \bar{\Delta},$$

$$Q_1 = Q_3 = Q_4 = Q_7 = Q_8 = Q_{13\sim18} = Q_{20\sim23} = Q_{25} = Q_{26} = 0,$$

$$R_3 = 1, \quad R_9 = -\bar{\omega}^2_u, \quad R_{10} = -\bar{\omega}^2_u \bar{x}_A, \quad R_{11} = \bar{\omega}^2_u, \quad R_{13} = 24\bar{\omega}^2_u \bar{\alpha} \bar{x}_A,$$

$$R_{16} = -12\bar{\omega}^2_u \bar{\alpha} \bar{x}_A^2, \quad R_{17} = -12\bar{\omega}^2_u \bar{\alpha} \bar{x}_A, \quad R_{18} = 12\bar{\omega}^2_u \bar{\alpha}, \quad R_{19} = 12\bar{\omega}^2_u \bar{\alpha} \bar{x}_A^2,$$

$$R_{20} = -12\bar{\omega}^2_u \bar{\alpha}, \quad R_{21} = -4\bar{\omega}^2_u \bar{\alpha}, \quad R_{24} = \left(\frac{\bar{\omega}^2_u \bar{x}_A}{6} - 4\bar{\omega}^2_u \bar{\alpha} \bar{x}_A^3 \right),$$

$$R_{26} = 4\bar{\omega}^2_u \bar{\alpha}, \quad R_{27} = -12\bar{\omega}^2_u \bar{\alpha} \bar{x}_A^2, \quad R_{31} = -\frac{\bar{l}_A}{2}, \quad R_{33} = -\frac{\bar{l}_A}{2},$$

$$R_1 = R_2 = R_{4\sim8} = R_{12} = R_{14} = R_{15} = R_{22} = R_{23} = R_{25} = R_{28\sim30} = R_{32} = 0,$$

$$S_4 = 1, \quad S_{10} = -\bar{\omega}^2_{\theta_A}, \quad S_{12} = \left(\bar{\omega}^2_{\theta_A} + \frac{3}{2} \bar{\omega}^2_{PD} \right), \quad S_{24} = -4\bar{\omega}^2_{\theta_A} \bar{\Delta},$$

$$S_{28} = -12\bar{\omega}^2_{\theta_A} \bar{\Delta}, \quad S_{29} = 12\bar{\omega}^2_{\theta_A} \bar{\Delta}, \quad S_{30} = \left(4\bar{\omega}^2_{\theta_A} \bar{\Delta} - \frac{1}{4} \bar{\omega}^2_{PD} \right),$$

$$S_{35} = -\frac{3}{2\bar{l}_A}, \quad S_{1\sim3} = S_{5\sim9} = S_{11} = S_{13\sim23} = S_{25\sim27} = S_{31\sim34} = 0.$$

Appendix C

$$P_1 = 1, \quad P_5 = \xi_y, \quad P_6 = \left(\frac{\xi_y \bar{l}_1}{4} - \frac{\xi_y \bar{l}_2}{4} \right), \quad P_9 = 1, \quad P_{10} = \frac{\bar{l}_1 - \bar{l}_2}{2}, \quad P_{11} = 0,$$

$$P_{13} = 0, \quad P_{14} = 0, \quad P_{15} = 0, \quad P_{16} = 6(\bar{\beta}\bar{l}_1 - \bar{\beta}\bar{l}_2), \quad P_{17} = 0, \quad P_{18} = 0,$$

$$P_{19} = 0, \quad P_{20} = 0, \quad P_{21} = 4\bar{\beta}, \quad P_{22} = 0, \quad P_{23} = (-\bar{\beta}\bar{l}_1 + \bar{\beta}\bar{l}_2),$$

$$P_{24} = (2\bar{\beta}\bar{l}_1^3 - 2\bar{\beta}\bar{l}_2^3) - \frac{\bar{l}_1 - \bar{l}_2}{12}, \quad P_{25} = 0, \quad P_{26} = 0, \quad P_{27} = 6(\bar{\beta}\bar{l}_1{}^2 + \bar{\beta}\bar{l}_2{}^2),$$

$$Q_2 = 1, \quad Q_5 = (\xi_{\theta_B} \bar{l}_1 - \xi_{\theta_B} \bar{l}_2), \quad Q_6 = (\xi_{\theta_B} \bar{l}_1{}^2 + \xi_{\theta_B} \bar{l}_2{}^2), \quad Q_9 = \bar{\omega}^2_{\theta_B} \bar{l}_1 - \bar{\omega}^2_{\theta_B} \bar{l}_2,$$

$$Q_{10} = \bar{\omega}^2_{\theta_B} (\bar{l}_1^2 + \bar{l}_2^2), \quad Q_{11} = 0, \quad Q_{12} = 0, \quad Q_{16} = 12\bar{\omega}^2_{\theta_B} \bar{\beta}(\bar{l}_1^2 + \bar{l}_2^2), \quad Q_{19} = 0,$$

$$Q_{21} = 4\bar{\omega}^2_{\theta_B} \bar{\beta}(\bar{l}_1 + \bar{l}_2), \quad Q_{24} = -\frac{2}{3} \bar{\omega}^2_{\theta_B} (\bar{l}_1^2 + \bar{l}_2^2) + 4\bar{\omega}^2_{\theta_B} \bar{\beta}(\bar{l}_1^4 + \bar{l}_2^4),$$

$$Q_{27} = \bar{\omega}^2_{\theta_B} \frac{-\bar{l}_1 + \bar{l}_2}{2} + 12\bar{\omega}^2_{\theta_B} \bar{\beta}(\bar{l}_1{}^3 + \bar{l}_2{}^3).$$

References

1. J. P. Den Hartog, *Mechanical Vibration* (McGraw-Hill, 1947).
2. A. F. Vakakis and S. A. Paipetis, The effect of a viscously damped dynamic absorbers on a linear multi-degree-of-freedom system, *J. Sound Vibr.* **105** (1986) 49–60.
3. Asustek Computer Inc., Dynamic damping system for disk drives, *Japan Patent*, No. 2, 951, 943 (1999) (in Japanese).
4. L. Zuo and S. A. Nayfeh, Minimax optimization of multi-degree-of-freedom tuned-mass dampers, *J. Sound Vibr.* **272** (2004) 893–908.
5. J. L. Almazán *et al.*, A bidirectional and homo-geneous tuned mass damper: A new device for passive control of vibrations, *Eng. Struct.* **29** (2007) 1548–1560.
6. Y.-R. Wang and T.-H. Chen, The vibration reduction analysis of a nonlinear rotating mechanism deck system, *J. Mech.* **24** (2008) 253–266.
7. Y.-R. Wang and M.-H. Chang, On The vibration reduction of a nonlinear support base with dual-shock-absorbers, *J. Aeronaut. Astronaut. Aviation, Series A* **42** (2010) 179–190.
8. Y.-R. Wang and H.-S. Lin, Stability analysis and vibration reduction for a two-dimensional nonlinear system, *Int. J. Struct. Stab. Dynam. (IJSSD)* **13**(5) (2013) 1350031-1–1350031-30.
9. E. Matta and A. De Stefano, Robust design of mass-uncertain rolling-pendulum TMDs for the seismic protection of buildings, *Mecha. Syst. Signal Process.* **23** (2009) 127–147.
10. I. Nagasaka, Y. Ishida, T. Koyama and N. Fujimatsu, Vibration suppression of a helicopter fuselage by pendulum absorbers: Rigid-body blades with aerodynamic excitation force, *J. Syst. Design Dynam.* **2** (2008) 1230–1238.
11. S.-T. Wu, Active pendulum vibration absorbers with a spinning support, *J. Sound Vibr.* **323** (2009) 1–16.
12. S.-T. Wu, Y.-R. Chen and S.-S. Wang, Two-degree-of-freedom rotational-pendulum vibration absorbers, *J. Sound Vibr.* **330** (2011) 1052–1064.
13. S.-T. Wu and P.-S. Siao, Auto-tuning of a two-degree-of-freedom rotational pendulum absorber, *J. Sound Vibr.* **331** (2012) 3020–3034.
14. A. Vyas and A. K. Bajaj, Dynamics of autoparametric vibration absorbers using multiple pendulums, *J. Sound Vibr.* **246** (2001) 115–135.
15. A. H. Nayfeh, *Introduction to Perturbation Techniques* (Wiley-Interscience, New York, 1981), pp. 107–131.
16. Z. Ji and J. W. Zu, Method of multiple scales for vibration analysis of rotor–shaft systems with non-linear bearing pedestal model, *J. Sound Vibr.* **218** (1998) 293–305.
17. C. P. Chao, C. K. Sung and C. C. Wang, Dynamic analysis of the optical disk drives equipped with an automatic ball balancer with consideration of torsional motions, *J. Sound Vibr.* 246 (2001) 115–135.